Technical Report Documentation Page

1. Report No. **FHWA/NC/2010-14**	2. Government Accession No.	3. Recipient's Catalog No.
4. Title and Subtitle Satellite Remote Sensing of Submerged Aquatic Vegetation Distribution and Status in the Currituck Sound, NC		5. Report Date November 1, 2012
		6. Performing Organization Code
7. Author(s) Dr. Stacy A.C. Nelson and Brett M. Hartis		8. Performing Organization Report No.
9. Performing Organization Name and Address Center for Earth Observation and Geospatial Sciences, Department of Forestry and Environmental Resources, North Carolina State University, Raleigh, NC		10. Work Unit No. (TRAIS)
		11. Contract or Grant No. 2010-14
12. Sponsoring Agency Name and Address North Carolina Department of Transportation Research and Analysis Group 1 South Wilmington Street Raleigh, North Carolina 27601		13. Type of Report and Period Covered Final Report 08/16/2009 - 09/15/2012
		14. Sponsoring Agency Code MA-2009-08
Supplementary Notes:		

16. Abstract

Submerged Aquatic Vegetation (SAV) is an important component in any estuarine ecosystem. As such, it is regulated by federal and state agencies as a jurisdictional resource, where impacts to SAV are compensated through mitigation. Historically, traditional detection methodologies have been proven to be ineffective or inappropriate for SAV mitigation over very large areas. These tasks are further complicated in that the location and density of SAV can change from year to year depending on variances in weather and water quality. Satellite remote sensing holds great promise for providing a labor and cost-effective means of monitoring and quantifying SAV distribution. For this analysis, sensor specific models based on multinomial logit procedures proved to be the best approach for predicting SAV presence or absence. No models could be developed for low distribution occurrence categories due to a low ratio of events to non-events. Statistical automated selection methods were developed to produce the final models we selected for each sensor. The use of the automated best-subsets method allowed for exploration of a number of potential candidate models based on the number of variables input in the model. The automated stepwise selection method led to the final, most reasonable model as decided upon in the best-subset procedure. For a variable to enter into or remain in the model, a p-value of <0.01 was necessary. A model was considered fit if the Hosmer and Lemeshow test yielded an insignificant difference in groups ($p>0.05$). Sensor specific models were developed for both the Quickbird and Worldview-II sensors, however LANDSAT 5 specific models were inconclusive largely due to quality of the data.

17. Key Words Remote Sensing, Monitoring, Sensors, Mapping, Mitigation, Spatial Modeling, Statistical Modeling, GIS	18. Distribution Statement		
19. Security Classif. (of this report) Unclassified	20. Security Classif. (of this page) Unclassified	21. No. of Pages 77	22. Price

Form DOT F 1700.7 (8-72) **Reproduction of completed page authorized**

DISCLAIMER

The contents of this report reflect the views of the author(s) and not necessarily the views of the University. The author(s) are responsible for the facts and the accuracy of the data presented herein. The contents do not necessarily reflect the official views or policies of either the North Carolina Department of Transportation or the Federal Highway Administration at the time of publication. This report does not constitute a standard, specification, or regulation.

Table of Contents

Table of Contents (Concluded)

List of Tables

List of Figures

List of Equations

List of Abbreviations

APES	**Albemarle-Pamlico Estuary System**
D	**Depth**
DN	**Digital Number**
IDW	**Inverse Distance Weighted**
LOGIT	**Logistic Regression**
MYSPIC	**Myriophyllum spicatum**
NAGUAD	**Najas guadalupensis**
NCDOT	**North Carolina Department of Transportation**
POPERF	**Potamogeton perfoliatus**
QB	**Quickbird**
RUMAR	**Ruppia maritime**
SAS EG	**SAS Enterprise Guide**
SAV	**Submerged Aquatic Vegetation**
SD	**Secchi Depth**
STPECT	**Stuckenia pectinata**
VAAMER	**Vallisneria americana**
WQ	**Water Quality**
WV-II	**Worldview-II**

1.0 INTRODUCTION

Submerged Aquatic Vegetation (SAV) is an important component in any estuarine ecosystem. As such, it is regulated by federal and state agencies as a jurisdictional resource, where impacts to SAV are compensated through mitigation. The North Carolina Department of Transportation (NC DOT) projects in the coastal area have the potential to impact SAV. Preparation of environmental documentation includes the identification of presence or absence of SAV in the project areas. Upon completion of avoidance and minimization protocols, compensatory mitigation is addressed. Historically, traditional wetland mitigation methodologies have been proven to be ineffective or inappropriate for SAV mitigation. These tasks are further complicated in that the location and density of SAV can change from year to year depending on variances in weather and water quality.

The NCDOT desires to understand trends in the presence or absence of SAV in coastal areas of North Carolina. This information will provide NC DOT and regulatory agencies with information necessary to realistically assess impacts to SAV from proposed project, and to determine appropriate avoidance, minimization, and compensatory mitigation alternatives. The dynamics (unpredictable presence or absence) of the SAV can lead to unintentional violations, as well as, over mitigating for the resource.

Large scale submerged aquatic vegetation (SAV) surveys are rarely possible, even though effective SAV management depends in part on understanding the coverage and abundance of SAVs, the growth forms present and/or the species present. This lack of survey data is largely due to the expense and challenges associated with sampling SAVs. Assessments are further complicated in regions covering thousands of hectare. For example, the Currituck Sound represents the northernmost sound along the Atlantic coast of North Carolina. This shallow inlet has a surface area of 39,600 ha (396 km^2) and a mean depth of 1.6 m (Wicker and Endres 1995). Inventorying this large of an area becomes cost-, time-, and labor-prohibitive using traditional field sampling techniques such as sampling along transects, within quadrants, or subsampling randomly-stratified lake points. Although these techniques can give good estimates of local SAV biomass and species composition at selected sites within a water body, these methods cannot capture whole-area plant biomass/cover or the patchy distribution of aquatic SAVs in an entire water body (Zhang, 1998). Remote sensing has the potential to be an important tool to obtain survey information on SAVs within large geographic areas (Valley et al., 2005; Vis et al., 2003).

Typically, remote sensing has been used to measure SAV cover by the labor-intensive process of mapping SAV areal distributions along coastal margins using visual interpretations of aerial photographs (Orth and Moore, 1983; Marshall and Lee, 1994). Unfortunately, this approach has limited applicability for assessing SAV distributions in regions with extensive, non-linear water bodies. Therefore, an approach that can accommodate larger areas is needed for regional water body monitoring of SAVs. One approach is to use high resolution satellite images, such as Digital Globe's Quickbird and Worldview-II satellite imagery. The two sensors currently have the highest commercially available spatial resolution available (2.44 m and 2.0 m multispectral

respectively) and possess the capability of synoptically capturing large areas within a single image (272 km^2). Although Quickbird and Worldview-II, like their Landsat predecessor, were primarily designed for detecting land features, recent improvements provide better spatial and spectral resolutions that may be applicable for aquatic studies (Zilioli, 2001). However, satellite remote sensing of aquatic SAVs, especially submersed SAVs, has been less studied than terrestrial vegetation because of the difficulties inherent in interpreting reflectance values of water (Penuelas et al., 1993; Lehmann and Lachavanne, 1997). For example, clear water provides little atmospheric reflectance and either absorbs or transmits the majority of incoming radiation (Lillesand and Kiefer, 1994; Verbyla, 1995). As a result, researchers have used remotely sensed data to detect primarily emergent vegetation or dense homogenous clusters of submersed vegetation (Ackleson and Klemas, 1987; Armstrong, 1993). Despite the potential limitations of using current sensors such as Quickbird and Worldview-II to detect submersed aquatic SAVs, more research is clearly needed to determine whether these sensors can be used to assess SAV abundance and distribution across a large geographical region.

Additionally, water body characteristics may need to be taken into consideration when attempting to remotely sense SAVs. For example, several studies have shown that remotely sensed images can measure characteristics such as chlorophyll, Secchi disk transparency, and suspended sediments (see Lathrop and Lillesand, 1986; Jensen et al., 1993; Narumalani et al., 1997; Lillesand et al., 1983; Khorram and Cheshire, 1985; Dekker and Peters, 1993; Kloiber et al., 2000; Nelson et al., 2003), all of which may influence the detection of SAVs, especially submersed SAVs. Water bodies within a region can vary widely in several of the above characteristics, which can also influence how aquatic SAVs are remotely sensed. For example, because water color and water depth may influence the sensor's ability to detect SAVs, it may be necessary to incorporate such factors into predictive models of aquatic SAVs. Water depth has been successfully incorporated into models to detect submersed SAVs using sensors such as Landsat in smaller bodies of water (Raitala and Lampinen, 1985; Ackleson and Klemas, 1987; Armstrong, 1993; Narumalani et al., 1997; Nelson et al., 2006). However tremendous potential still exists in the capacity of high resolution satellite imagery to detect submersed SAVs within a large region, such as the Currituck Sound of North Carolina.

2.0 PROJECT AREA

The Currituck Sound is located in the Northeastern most corner of North Carolina and makes up the northern arm of the Albemarle-Pamlico Estuary System (APES), the second largest estuary in the United States, thus making it one of the most important wildland habitats in the nation. The Sound stretches approximately 30 miles from North to South and 3 to 8 miles from east to west dependent upon location. On its northernmost end the Sound extends to Back Bay, Virginia and into the Albemarle -Chesapeake Canal. To the south, it joins the Albemarle Sound and the rest of the APES system. The freshwater inputs to Currituck Sound include North Landing River and Northwest River, both with headwaters in the Great Dismal Swamp of North Carolina. Back Bay also contributes water (both salt and fresh) into the Sound through shallow water channels. Inputs of brackish water from Federal canals also might influence the salinity of Currituck Sound. The sound is separated from the Atlantic Ocean by a narrow strip of barrier islands known as the outer banks which are no more than a mile wide. The Sound has an average depth of 5 feet (1.52 meters) and maximum depth of approximately 13 feet (3.96 meters). Water level

fluctuations in Currituck Sound are a product of constantly changing wind. The Sound stretches through two counties; Dare and Currituck, with level or slightly sloping terrain that drains into the Currituck Sound.

The survey area spans the mid-Currituck portion of the Currituck Sound encompassing the Currituck County mainland and outer banks as well as the Dare County outer banks (figure 2.1). The project area is approximately 13 miles long by 5 miles wide stretching from just south of Corolla to Duck on the eastern side and Parker's creek to Webster's creek on the western side.

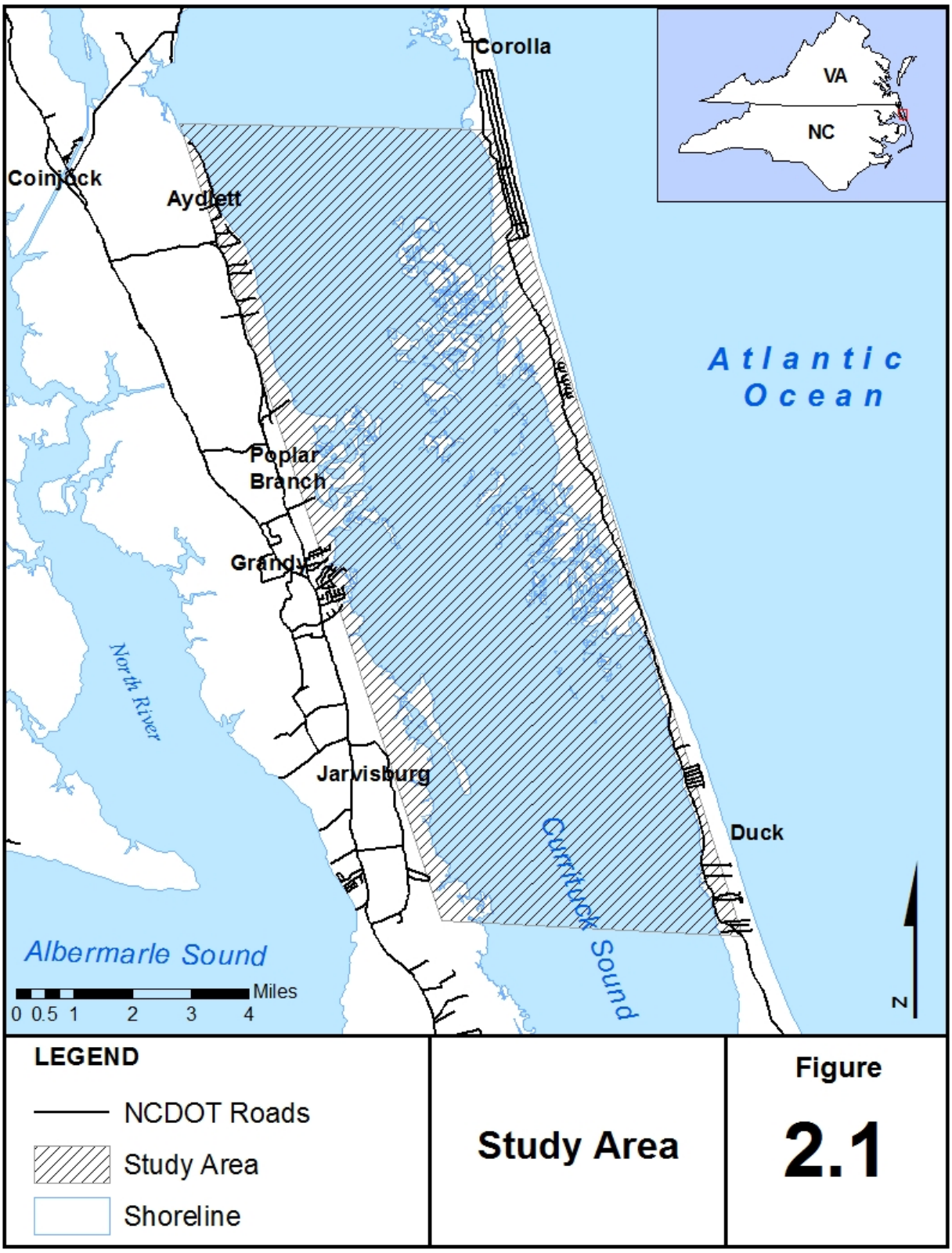

Figure 2.1. Study area for SAV sampling and remote sensing

3.0 PROJECT DESCRIPTION

3.1. Objectives

The objectives in this study are: (1) to determine if different levels of aquatic plant cover and plant types (overall littoral SAVs (i.e. total presence/absence) can be detected using the commercially available Quickbird and Worldview-II satellite sensors or free LANDSAT 5 data and (2) to determine if predictions of SAV abundance and distribution can be improved by including limnological characteristics (Secchi disk depth, salinity, sediment type, and water depth) and water quality (Total nitrogen, total phosphorus, etc) in the models. Secondary objectives of this study are to identify existing beds of SAV and to determine the spatial extent and status with the use of currently accepted survey techniques and remote sensing.

The hypothesis of this study is that satellite remote sensing will provide an effective means of detecting SAV and the inclusion of the additional water clarity and quality characteristics will strengthen relationships between SAV cover and sensor spectral values.

3.2. SAV sampling

The Currituck sound was sampled during the summer-stratified season and peak plant biomass (June –September). SAVs were sampled using a modification of the point intercept method (Madsen, 1999). The sound was gridded into 174 equidistant points that were sampled three times during the summer-stratified season: Sample 1 (06/14/10-07/13/10), Sample 2 (07/24/10-08/07/10) and Sample 3 (09/03/10-09/06/10). Initial findings allowed for reduction of sample points as locations with an initial depth of 10 feet (3.05 meters) or greater identified in sample 1 were deemed too deep for plant growth. Also, points found to be on island structures were removed as SAVs would be unable to establish growth on such terrestrial features. Therefore, only points in the littoral zone of the Sound remained for sample 2 (N of 117). Sample 3 was reduced to 31 points given time restraints and served solely as a validation dataset. The sample points were located in the field using a Magellan MobileMapper CX professional grade GPS unit. At each point, water depth was measured and plant composition assessed by recording plant presence and plant cover at each site. This was accomplished by qualitatively assigning a 'plant cover level' for each category. Plant cover was assessed at each point for an area of 10mx10m by utilizing a two-sided sampling rake thrown in four cardinal directions from the point of anchor. A locational error of +/- 5 feet (1.52 meters) was thought to be obtained through constant repositioning. Plant cover levels were initially separated into 10% field interval categories ranging from 0 (0%) to a level of 10 (91-100%). These levels were then combined in the lab to represent four levels most likely to be discernible by each sensor: 0 (0–20% plant cover), 1 (21–40% plant cover), 2 (41–80% plant cover), and 3 (81–100% plant cover). An additional binomial category of total littoral zone plant cover was developed by combining the four levels recorded for each plant category at each point. This category captures littoral plant presence or absence at each point by assigning each site either a 0 (0–20% plant cover) or a 1 (21–100% plant cover). All values of plant cover less than 20% are thought to be undetectable by most currently available sensors and were therefore assigned a value of "0" or absence (Nelson et al. 2003). For non-model purposes, a littoral percent plant cover was calculated as the total number of points sampled with any plant category greater than level 0 (i.e., >1% cover at an

individual site), divided by the total number of points in the littoral zone. The littoral zone is defined as <2 m water depth (figure 3.1). Sites with a depth of >2 m will be regarded as pelagic where it will be assumed that reflectance of the water column would dominate the reflectance spectra necessary for submersed plant detection by the satellite sensor (Ferguson and Korfmacher 1997).

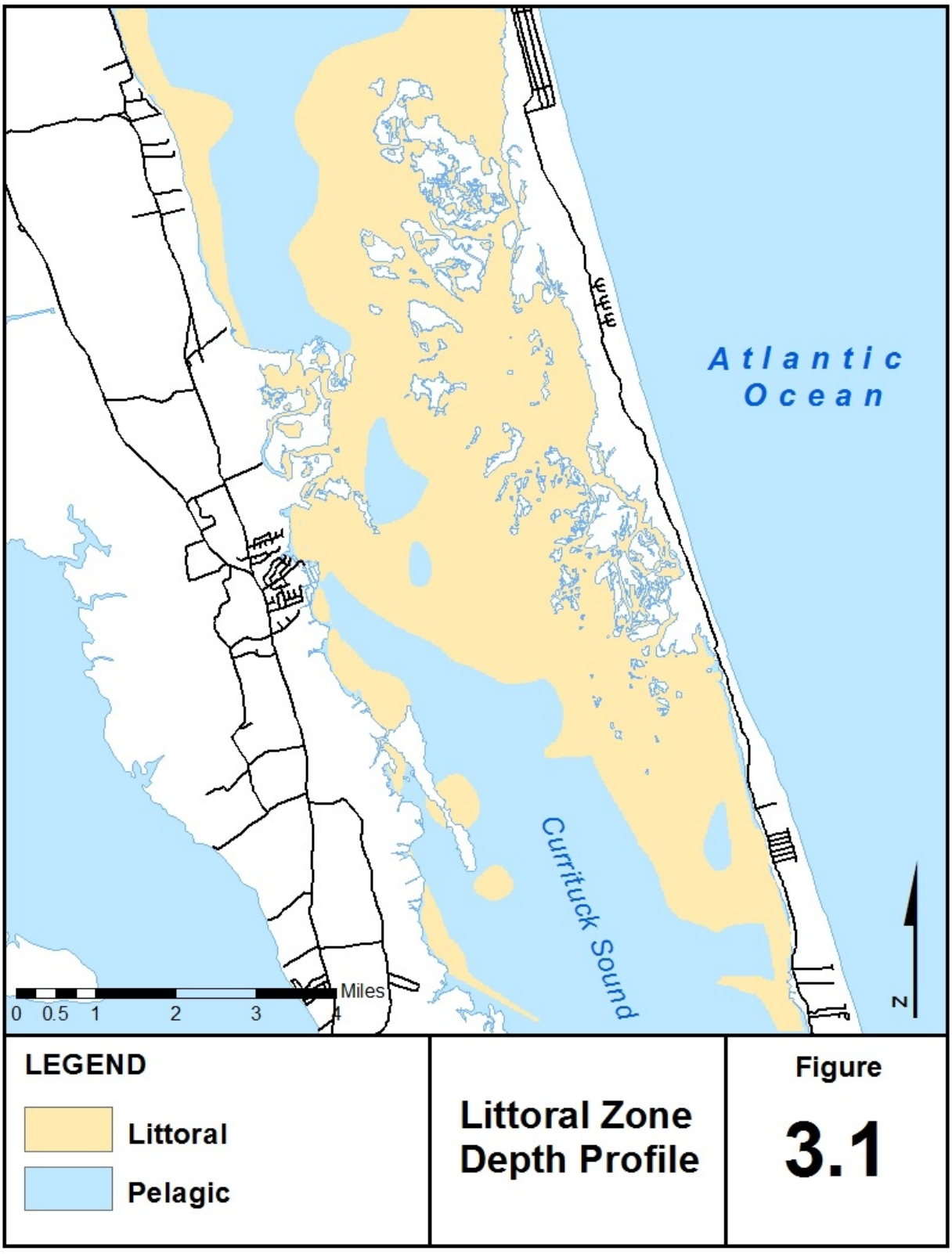

Figure 3.1. Littoral zone of study area as estimated through summer 2010 SAV sampling

3.3. Water Quality Characteristics

Water clarity was estimated using a 20 cm diameter Secchi disk. Secchi depth was determined by averaging two measurements taken over the shady side of the boat during SAV sampling. Pelagic water samples were taken from the deepest area of the study area (sample point 169 = 10.5 feet) directly adjacent to multiple aggregated sampling areas for comparison. A temperature profile was also established using an onboard thermometer during all SAV sampling. Salt content of the water was determined with the use of a handheld refractometer by taking four readings over the side of the boat and averaging. Finally, sediment type estimates were developed by collecting samples during each SAV sampling run in the littoral zone of the aggregated sampling areas with a bottom grab from directly under the boat. Lake sediments were categorized into ten different types that represent identified soil texture. These were clay, clay loam, loam, loamy sand, sand, sandy clay loam, sandy loam, silt, silt clay, and silt loam.

For water quality estimations, a representative dataset was developed from which to test water quality. This representative dataset was then interpolated to provide water quality at each SAV sample point. Water quality parameters identified below were tested between SAV sampling runs: WQ sample 1 (07/08/10-07/23/10) and WQ sampling 2 (08/08/10-08/14/10). Water quality parameters were estimated with the use of the LaMotte SMART® Spectro Spectrophotometer. Measures of water quality included total nitrogen, total phosphorus, ammonia nitrogen, Nitrate-N, Color, Dissolved Oxygen, Nitrite-N, Phosphate-P and pH. Dissolved Oxygen, pH, and Color were all derived in the field using procedures designated for testing by LaMotte. All other samples were collected into 32 ounce sampling containers, preserved using procedures specified by LaMotte and transferred back to the lab packed in ice. Samples taken back to the lab were processed the same day as collection. Total nitrogen was determined using a persulfate digestion followed by second derivative spectroscopy (Crumpton et al., 1992). Total phosphorus was determined using a persulfate digestion (Menzel and Corwin, 1965) followed by standard colorimetry (Murphy and Riley, 1962). Ammonia nitrogen was determined using the reaction of Salicylate and ammonia in the presence of a chlorine donor and an iron catalyst which forms a blue indophenol dye. The concentration of which is proportional to the ammonia concentration in the sample. Nitrate-N concentration was determined using zinc to reduce nitrate to nitrite. The nitrite that was originally present, plus the reduced nitrate, reacts with chromotropic acid to form a red color in proportion to the amount of nitrate in the sample. Nitrite-N was determined using the compound formed by diazotization of sulfanilamide and nitrite which is coupled with N-(1-naphthyl)-ethylenediamine to produce a reddish purple color in proportion to the nitrite concentration. Phosphate-P concentrations were determined using an ammonium molybdate and antimony potassium tartrate reaction in a filtered acid medium with dilute solution of PO4. This reaction forms an antimony-phosphomolybdate complex. This complex is reduced to an intense blue colored complex by ascorbic acid. The color is proportional to the amount of phosphate present. All Water quality estimates were matched to images and SAV samples with acquisition and sample dates that most closely corresponded to water quality collection dates.

3.4 SAV Mapping using IDW Approach

In order to provide the NCDOT with maps of existing plant communities, an Inverse Distance Weighted (IDW) approach was utilized to map existing plant communities based solely on SAV point sampling. These maps were also developed to provide estimations of probable SAV distributions throughout the entirety of the Sound. The IDW approach is a deterministic method for multivariate interpolation (ArcMAP 10.0) and is based on the assumption that things that are close to one another are more alike than those that are farther apart. Thus, a weighting system was developed based on all SAV sample points and only their closes neighbors. The Spatial Analyst>Interpolation>IDW tool in ArcMap 10.0 was used to complete all interpolations. The sample points for each sampling run were used as the input point features with the SAV binomial or multinomial variable as the Z-value field. An output cell size of 30 meters and a power of 2 were used to increase the influence of the closest points and provide as much differentiation as possible. The IDW was based on a fixed search radius of 1300 meters to include all points adjacent (above, below, left, right or diagonal) to each point being interpolated. The output was a smooth continuous raster surface of potential existent SAV communities. These maps do not represent SAV distribution to actual scale however. The same procedure was used to map all other variables collected during SAV sampling in 2010.

3.5. Satellite imagery

Quickbird satellite imagery (2.44 m) and Woldview-II imagery (2.0m) were acquired from Digital globe and LANDSAT 5 imagery for the entire Mid-Currituck Sound study area and were matched to the SAV and water quality samples. Each sensor records spectral data based on the electromagnetic spectrum and records this data into spectral ranges known as bands. The Quickbird sensor is made up of four spectral bands: Band 1 (450-520 nm), Band 2: (520-600 nm), Band 3 (630-690 nm), and Band 4 (760-900). The Worldview-II sensor is made up of 4* spectral bands: Band 1 (450-510 nm), Band 2 (510-580 nm), Band 3 (630-690 nm) and Band 4 (860-1040 nm). The LANDSAT-5 sensor is made up of 7 bands: Band 1 (450-520 nm), Band 2 (520-600 nm), Band 3 (630-690 nm), Band 4 (760-900 nm), Band 5 (1550-1750 nm), Band 6 (1040-1250 nm) and Band 7 (2080-2350 nm). Band 6 was omitted from this study given its spectral range is not advantageous in vegetation studies. Each sensors characteristics are summarized in table 3.1. For band specific wavelengths, see tables 3.2 – 3.4.

Sensor	Spatial (m)	Spectral (nm)	Radiometric (bits)	Temporal (days)	Bands
Worldview-II	1.8-2.4	450-1040	11	3.7	4*
Quickbird	2.44-2.88	450-900	11	3.5	4
LANDSAT-5	30 (120 Band 6)	450-1250	8	7	7

Table 3.1. Sensor specifications for spatial, spectral, radiometric and temporal resolution. * Worldview-II currently contains 4 additional bands that were not assessed during this study

Worldview-II				
Band	1	2	3	4
Name	Blue	Green	Red	NIR
Spectrum Width (nm)	450 - 510	510 - 580	630 - 690	860 - 1040

Table 3.2. Multi-Spectral bands of the WorldVeiw-2 satellite sensor

Quickbird				
Band	1	2	3	4
Name	Blue	Green	Red	NIR
Spectrum Width (nm)	450 - 520	520 - 600	630 - 690	760 - 900

Table 3.3. Multi-Spectral bands of the Quickbird satellite sensor

LANDSAT 5 TM						
Band	1	2	3	4	5	7
Name	Blue	Green	Red	NIR	SWIR	SWIR-2
Spectrum Width (nm)	450 - 520	520 - 600	630 - 690	760 - 900	1550 - 1750	2080 - 2350

Table 3.4. Multi-Spectral bands of the LANDSAT 5 TM satellite sensor

Two Worldview-II, Two-Quickbird and five LANDSAT 5 images were acquired over the summer of 2010. Each image encompasses a portion or the entirety of the study area. Original images from each sensor are found in figures 3.1-3.5.

Worldview – II:

July 22nd, 2010 (Entire)
August 5th, 2010 (Partial)

Quickbird:

August 5th, 2010 (Partial – Not Applicable)
September 13th, 2010 (Entire)

LANDSAT-5:

April 20th, 2010 (Entire)
May 8th, 2010 (Entire)
July 11th, 2010 (Entire)
August 28th, 2010 (Entire)
September 13th, 2010 (Entire)

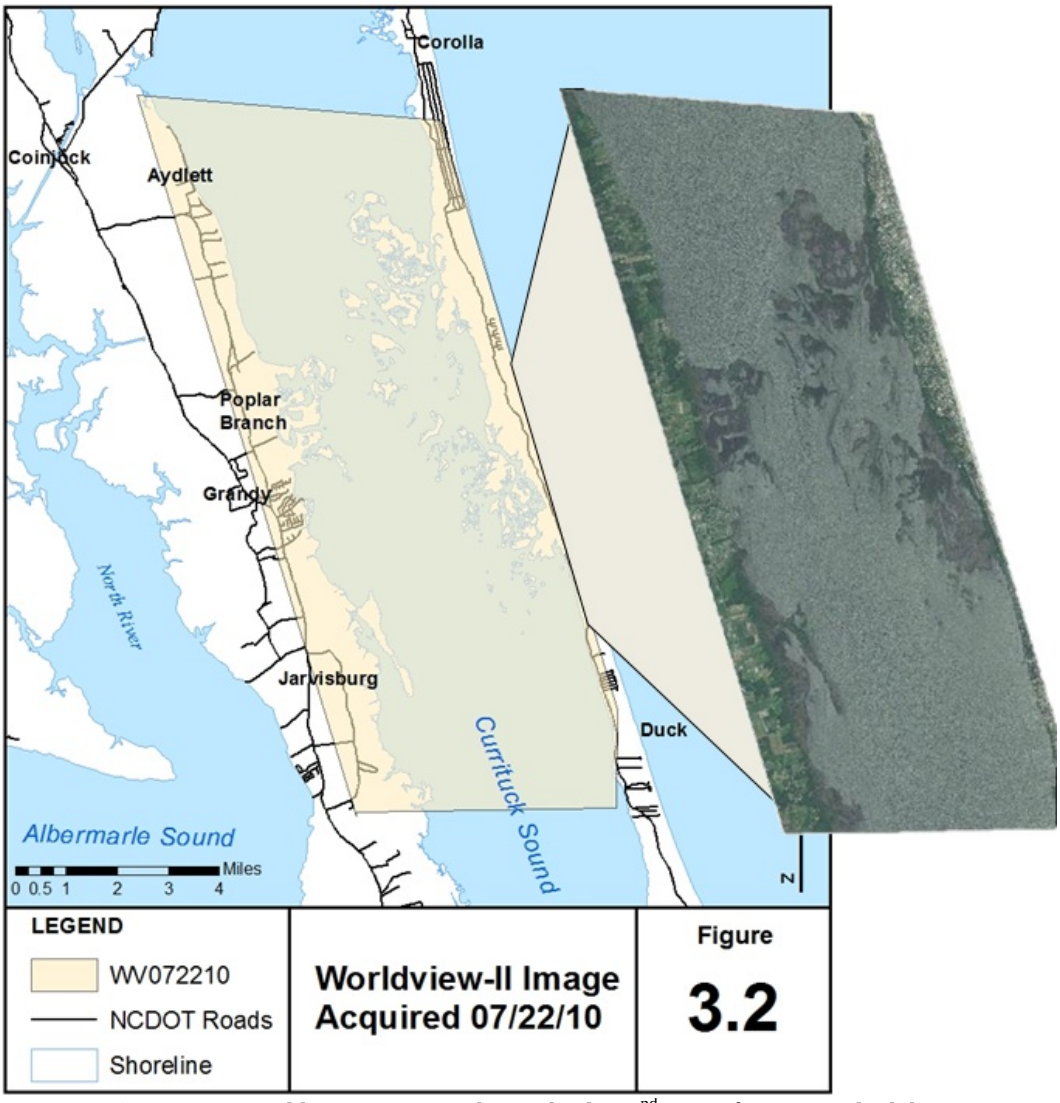

Figure 3.2. Worldview-II image obtained July 22nd, 2010 from Digital Globe.

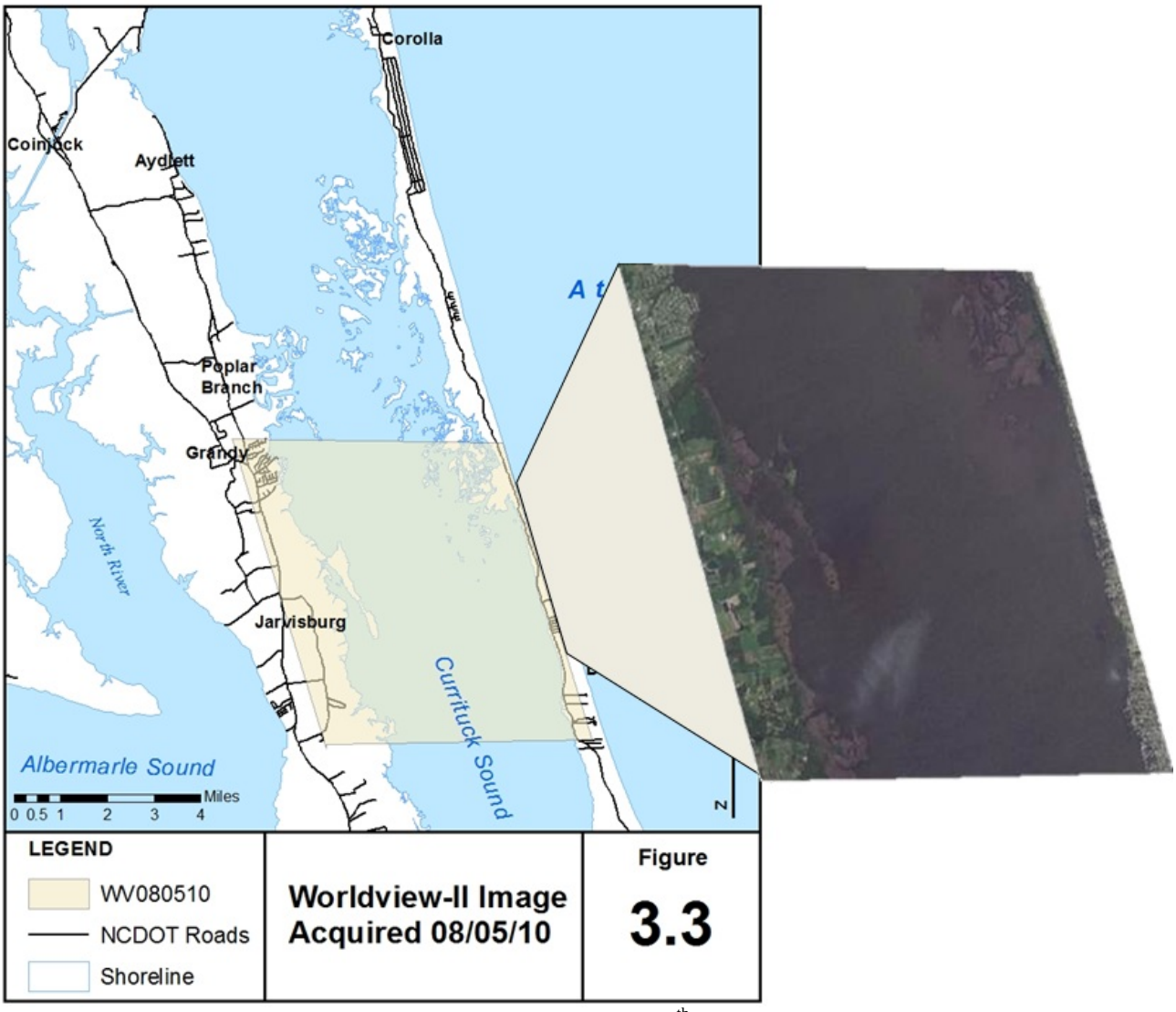

Figure 3.3. Worldview-II image obtained August 5th, 2010 from Digital Globe.

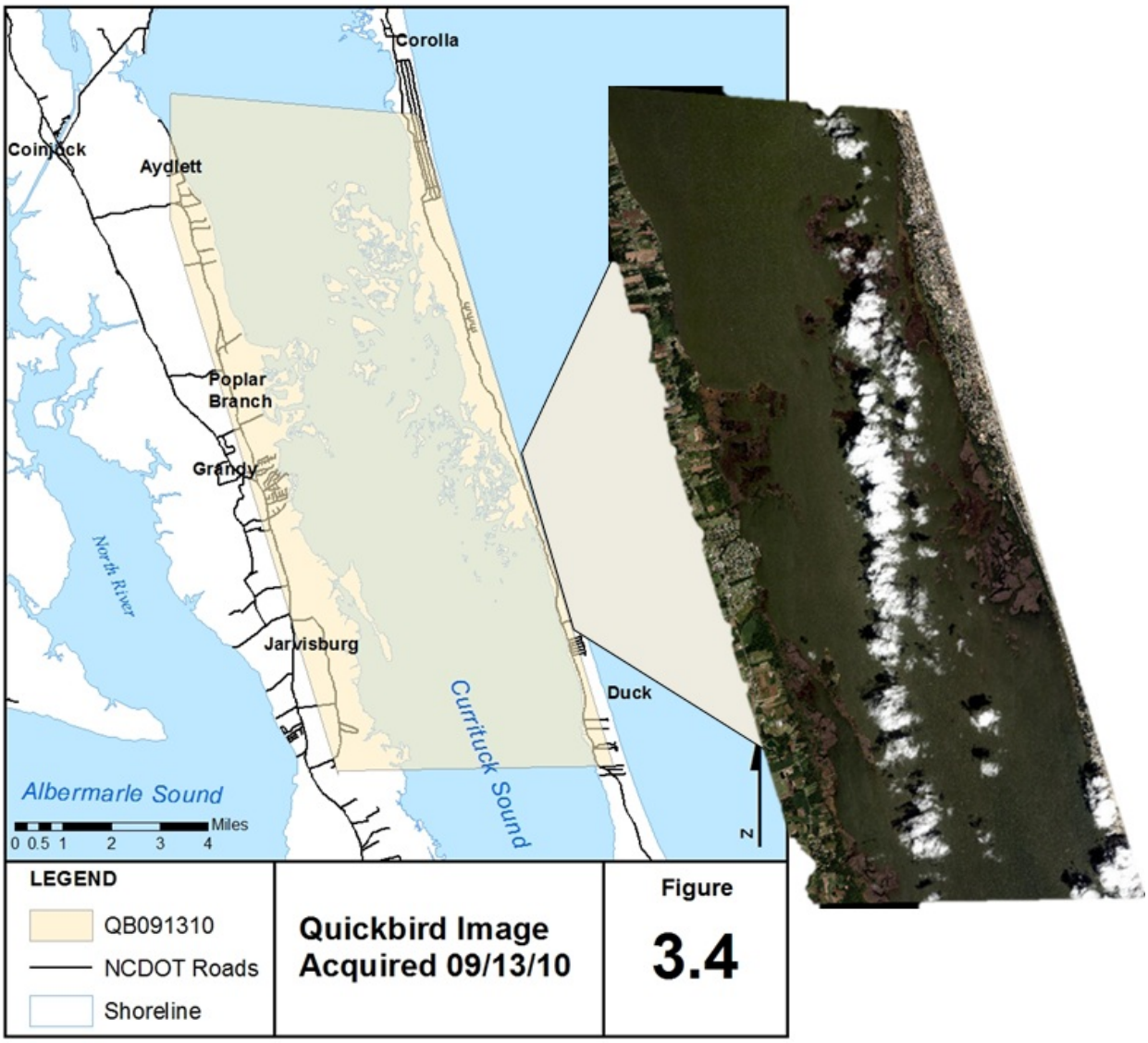

Figure 3.4. Quickbird image obtained September 13th, 2010.

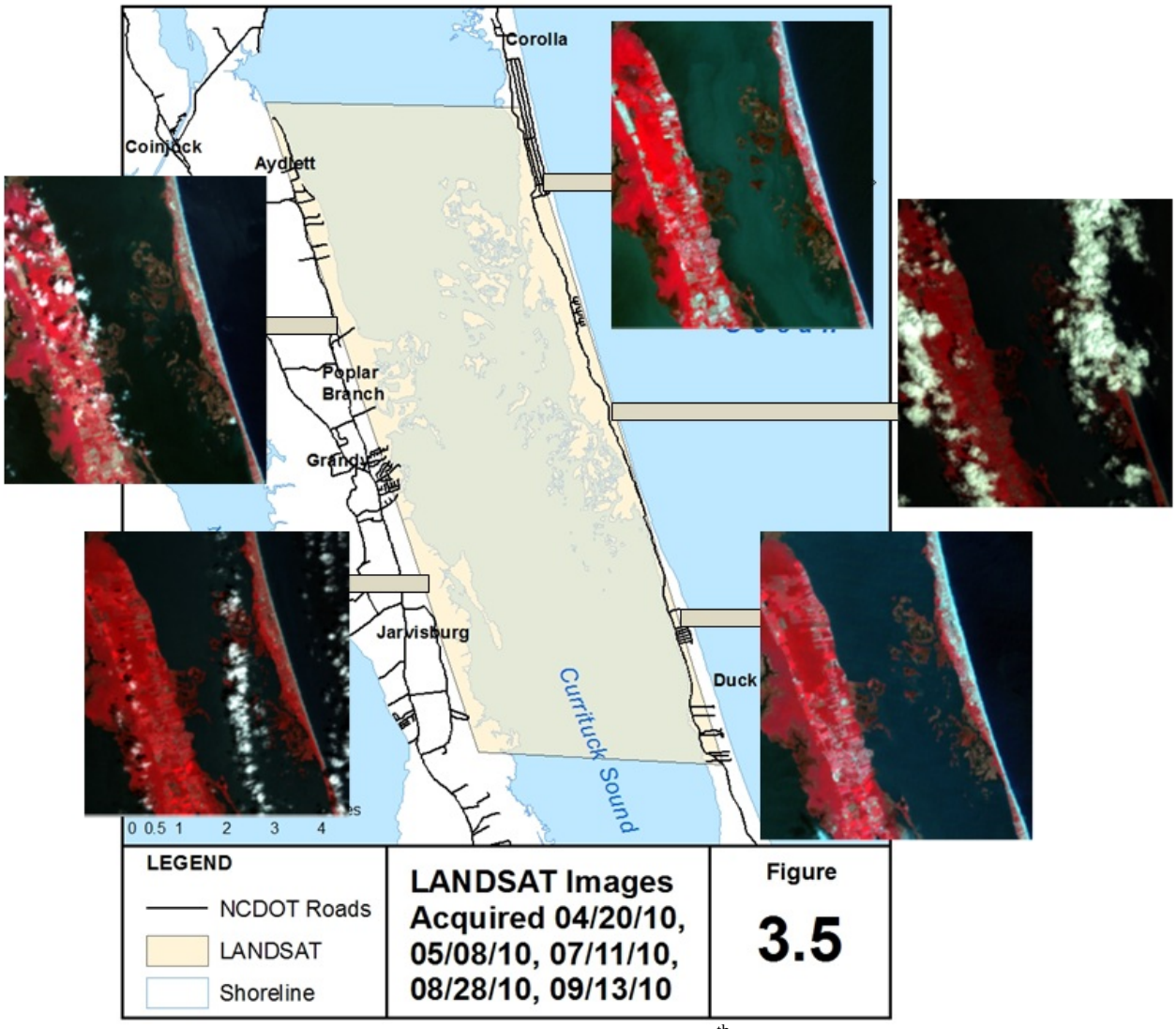

Figure 3.5. LANDSAT 5 ETM images obtained April 20th through September 13th, 2010

Image rectification and geoprocessing were conducted using ERDAS Imagine 2011 image processing software. Quickbird and Worldview-II images came already georectified, however visual inspection showed that further georeferencing was necessary for some images. Images taken on 09/13/10 (QB) and 08/05/10 (WV-II) were georeferenced to the Worldview-II image considered most spatially accurate using professional judgment (07/22/10). All imagery was georeferenced using a 1st order polynomial transformation with no less than 10 ground control points. Error was minimized to less than 1 pixel per transformation. All imagery was inspected for atmospheric differences occurring between scenes and histogram matching was completed when necessary. Due to the high occurrence of clouds in most images, a cloud removal masking technique was required to remove all pixels containing clouds or cloud shadows. All land features were masked out using similar masking techniques. Data points lying within pixels containing clouds, shadows or other interference were subsequently removed from the dataset before any statistical analyses were performed.

The spectral pixel values or digital number (DN) values for all single pixels containing the position of each sample point, using the field-recorded GPS coordinates, were extracted using the Spatial analyst>Extraction>Extract Multi Values to Points tool in ArcMap 10.0. DN values were extracted from each individual scene and combined with all SAV sampling data into one database file. Spectral DN values for the pelagic region (sample points with depth measurements >6 feet or 1.83 meters) were also extracted to analyze the relationship between pelagic zone sound characteristics and spectral values. Because the pelagic zone is more homogeneous than the littoral zone, the spectral DN values for all pixels within the pelagic zone of the aggregated sampling areas were averaged resulting in one pelagic spectral value. In turbid North Carolina coastal bodies of water, SAVs are unable to establish or grow in depths greater than 6 feet (1.83 meters) due to a lack of adequate sunlight (Ferguson and Korfmacher 1997). Thus, areas greater than 2 meters in depth were deemed "pelagic" for the purposes of this study. Given the high spatial resolution of the Worldview-II and Quickbird sensors, extraction of WV-II and QB DN values were based on a bilinear interpolation of the pixel containing each GPS sample point along with that pixels nearest neighbors and computed into an average spectral reflectance value. This was completed for Worldview-II and Quickbird to more closely replicate actual site sampling size of SAVs. LANDSAT 5 DN extraction was based solely on the single pixel containing the GPS sample point as LANDSAT imagery is of much coarser spatial resolution (30m) than both WV-II and QB.

Determination of outliers was completed using visual and statistical inspection of each DN value at each point. Any DN value identified as an outlier (> 1.5 x IQR) in SAS Enterprise Guide 4.2 (SAS EG) was ultimately inspected for atmospheric interference and removed upon confirmation. All images were inspected for points lying within previously masked clouds, along land, or within previously masked shadow areas eliminated in preprocessing and subsequent points were removed based on professional judgment. Points removed were deemed unusable in model development due to the high degree of influence from sources outside of the target. This procedure was completed for each image/ SAV sampling dataset combination. All spectral digital number values were independently and statistically evaluated for interference from atmospheric or sensor defects before attempting to develop a spectral model data set for each sensor.

3.6. Statistical analysis

The satellite imagery DN values and SAV data were analyzed using binomial and multinomial logistic regression (logit models) in SAS EG. Stepwise and best-subset regression techniques were used to fit individual and combined spectral bands to the sample data. All models also initially included water depth, secchi depth, salinity, temperature and estimated water quality parameters at each sampling point as an interaction term with each main effect variable (i.e. fitted spectral band or combined bands).

All image/SAV combined sampling data points not eliminated during outlier detection were included in all logit models for each sensor and combined models. The multinomial and binomial categories for plant cover and plant presence absence served as individual response variables for each logit model. The logit model uses the explanatory and interaction covariates to predict the probability that the response variable will take on a given value (SAS Institute Inc., 1995). The logit model expression is given where Y-hat is the estimated probability that the ith case is in a category (equation 3.1a) and u is the regular linear regression equation (equation 3.2b) where u is the response variable (binary or multinomial category) and X_1-X_k are the explanatory variables (Band DN, Depth, Secchi, etc) and B_1-B_k are the regression coefficients of X_1-X_k.

$$\hat{Y}_i = \frac{e^u}{1+e^u}$$

Equation 3.1a.

$$u = A + B_1X_1 + B_2X_2 + \cdots + B_KX_K$$

Equation 3.1b

For binomial logistic regression, the logit model indicates how the explanatory variable (DN values by band) affects the probability of the event (SAV presence/absence) being observed versus not being observed. For the multinomial logistic regression, probable outcomes of observations are calculated by analyzing a series of binomial sub models that represent the overall model's ability to predict each of the plant cover response variables. For all logit model analyses, the descending option was used to select the highest plant category level as the response variable reference (level 3 for plant cover and level 1 for littoral plant presence/absence). This selection ensures that the results will be based on the probabilities of modeling an event (SAVs present), rather than a non-event (SAVs not present).

Model fit was determined by examining the percent concordant values, the Wald test statistic, likelihood ratio, and score test. The percent concordant values provide an indication of overall model quality through the association of predicted probabilities and observed responses. These values are based on the maximum likelihood estimation of the percent of paired observations of which values differ from the response variable (Kleinbaum, 1994). Thus, the higher the predicted event probability of the larger response variable (based on the highest plant category level), the greater the percent concordant value will be. The Chi-square level of significance for the Wald test statistic, Likelihood ratio and score tests test the hypothesis that the coefficients of the independent variables are significantly different from zero by fitting the model using the intercept terms (Kleinbaum, 1994; Pampel, 2000). The Hosmer and Lemeshow Goodness of fit

test was used to determine the overall model goodness of fit. The Hosmer and Lemeshow Goodness of Fit test tests the null hypothesis that the data are generated by the model fitted by the researcher. The test divides subjects into deciles based on predicted probabilities, and then computes a chi-square from observed and expected frequencies (Hosmer and Lemeshow 2000). Then a probability (p) value is computed from the chi-square distribution with 8 degrees of freedom to test the fit of the logistic model. If the Hosmer and Lemeshow Goodness-of-Fit test statistic is .05 or less, the researcher will accept the null hypothesis that there is no difference between the observed and model-predicted values of the dependent. (This means the model predicts values significantly different from what they ought to be, which are the observed values). If the Hosmer and Lemeshow goodness-of-fit test statistic is greater than .05, as the researcher wants for well-fitting models, then the researcher will fail to reject the null hypothesis that there is no difference, implying that the model's estimates fit the data at an acceptable level.

To examine whether there were significant differences between data obtained from multiple images of the same sensor, individual-image logit models were developed. The model output and model coefficients from each image were compared using a two sample t-test to test for differences between the means of the model coefficients (log transformed). Resultant p-values for the paired variance and significance were determined at the 0.1 level. Insignificant results from these tests suggest that the means of the individual image data show no significant difference. Second, the means of the percent concordant values from the individual image data were compared. In this analysis, the absence of large differences between the data percent concordant values will support the validity of creating a sensor specific model across multiple images.

Logit models for individual images were used to examine whether various water quality characteristics helped improve predictions of plant cover using Quickbird, Worldview-II and LANDSAT 5 imagery. Ordinary least squares regression were used to regress each of the model coefficients from the individual image logit models against each of the measured water quality characteristics individually: Secchi depth, water depth, salinity, water temperature, sediment type, total nitrogen, total phosphorus, ammonia nitrogen, Nitrate-N, Color, Dissolved Oxygen, Nitrite-N, Phosphate-P and pH

3.7. LOGIT Model Validation

Model validation was accomplished using the results/output of logit predictive models and comparing those to outputs developed using SAV sampling data only. The validation was made by investigating point specific logit predictions and comparing them to point specific SAV sampling data of actual ground truthed data. An inverse distance weighted method was also used to interpolate values between points of both the logit predicted dataset and the SAV sampling produced dataset. The Inverse Distance Weighted approach is based on the assumption that things that are close to one another are more alike than those that are farther apart. To predict a value for any unmeasured location, IDW uses the measured values surrounding the prediction location. The measured values closest to the prediction location have more influence on the predicted value than those farther away. IDW assumes that each measured point has a local influence that diminishes with distance. It gives greater weights to points closest to the prediction location, and the weights diminish as a function of distance, hence the name inverse distance

weighted. IDW estimations were produced using the Inverse Distance Weighted procedure in ArcMAP's Spatial Analyst extension. Given the distance between points, only points adjacent to other points were utilized (fixed search neighborhood of <1300m) for IDW estimates and were based on a power function of p=2, which greatly reduces influence of points as distance increases. The logit values represented the cumulative probability of each sample point being each plant cover level (0, 1, 2, and 3) or littoral plant presence (0 or 1) within each plant category. The cumulative probability value of the logit was used to calculate the actual probability of each sample point being each plant cover level or plant presence. The actual probabilities were then averaged to determine the overall probability of sample points belonging in each plant cover level and plant category. All model outputs (SAV sampling IDWs and Logit model IDWs) were exported to ArcGIS to produce an SAV distribution and status analysis of the Currituck Sound per image based on points utilized for modeling. Separate maps were developed to show ALL points sampled during SAV sampling to give an entire sample area status and distribution without image based outliers removed.

4.0. RESULTS

4.1. Distribution of SAV

One objective of this study was to provide adequate information representative of the extent and distribution of SAV within the designated study area presented in figure 2.1. Vegetated areas were estimated using point specific data and the IDW approach. General SAV extent and distribution were classified into two categories by percent plant cover as determined during field sampling: Presence/Absence and Plant Density. Plant absence was defined as any point containing less than 1% of SAV and plant presence as 1% to 100% as present. (Note: For incorporation into the logistic regression model however, all points containing less than 20% plant coverage were considered absent based on the limitations of each sensor to detect plant levels less than 20%). During summer sampling, SAV was found to be present on average at 46% of all points sampled. Points designated as part of the littoral zone (<6.0 feet or 1.83 meters deep) demonstrated SAV presence at 69.46% of the sample points on average throughout summer sampling. SAV presence and absence per sampling set is demonstrated in figures 4.1.a and 4.1.b.

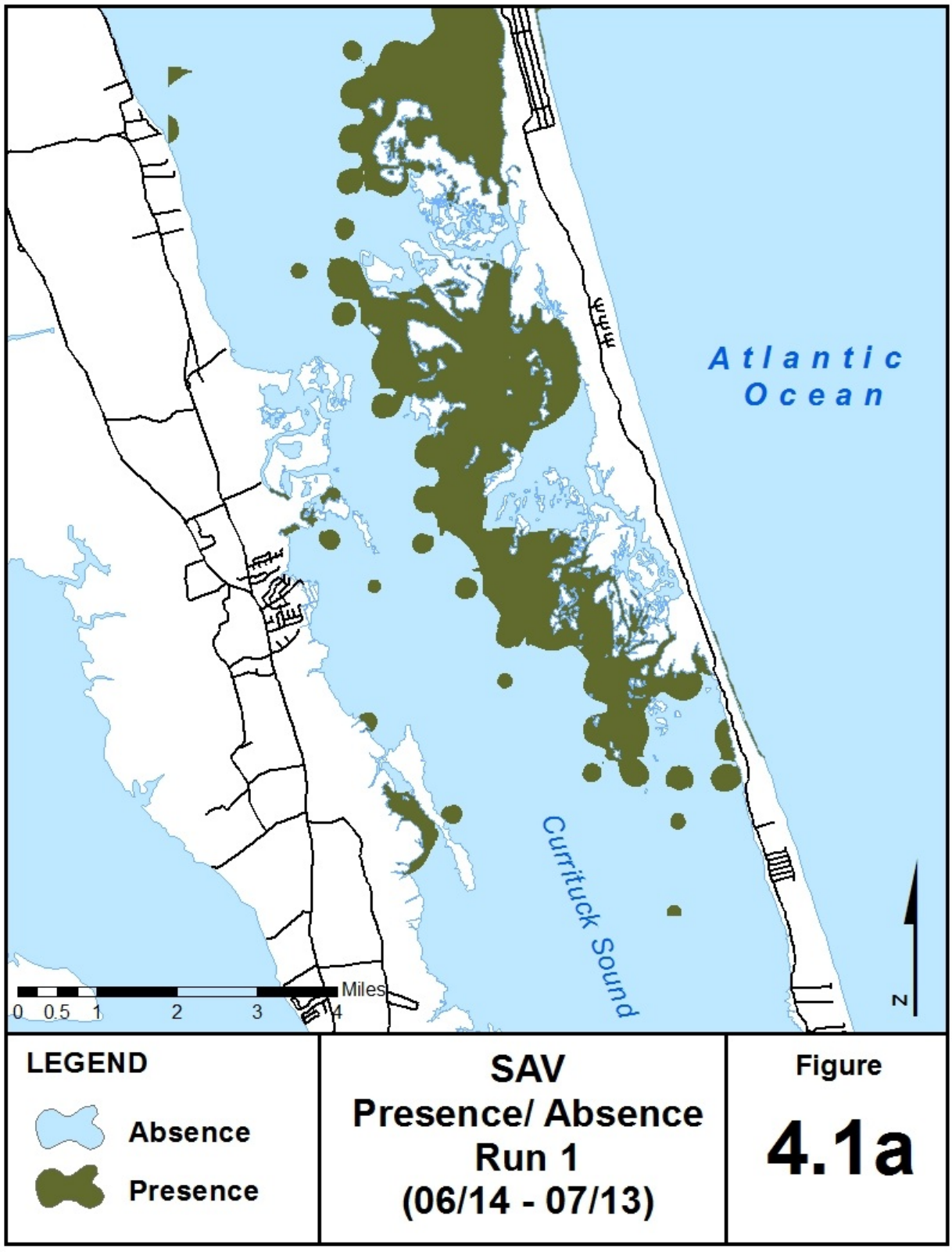

Figure 4.1a. SAV presence/absence for run 1. Absence = 0% plant coverage, Presence = 1-100% plant coverage

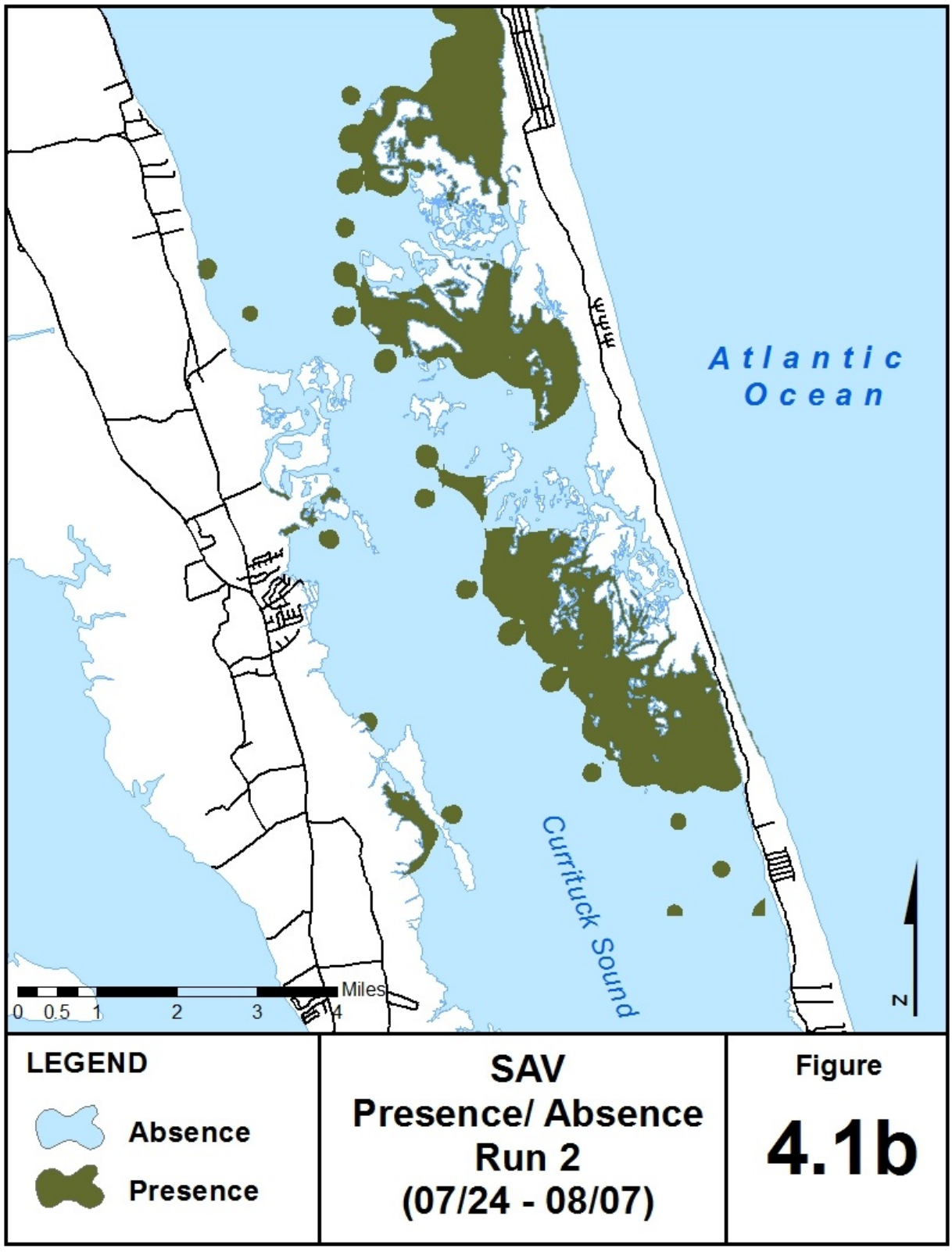

Figure 4.1b. SAV presence/absence for run 2. Absence = 0% plant coverage, Presence = 1-100% plant coverage

SAV spatial extent and distribution were also determined in terms of percent cover. Overall plant coverage in the littoral zone of the Currituck Sound for each sampling run is presented in figures 4.2a and 4.2b. Percent cover classes were separated into five main classes. These classes were 0 (<1%), 1 (1-20%), 2 (21-40%), 3(41-80%), and 4 (81-100%) based on overall plant coverage at each point. In terms of plant coverage categories, the majority (53.42%) of points sampled were devoid of plants, 24.36% of sample points fell into level 1 (>1%-20%), 11.11% into level 2 (21-40%), 7.69% of points into level 3 (41-80%) and 3.42% falling into level 4 (81-100%).

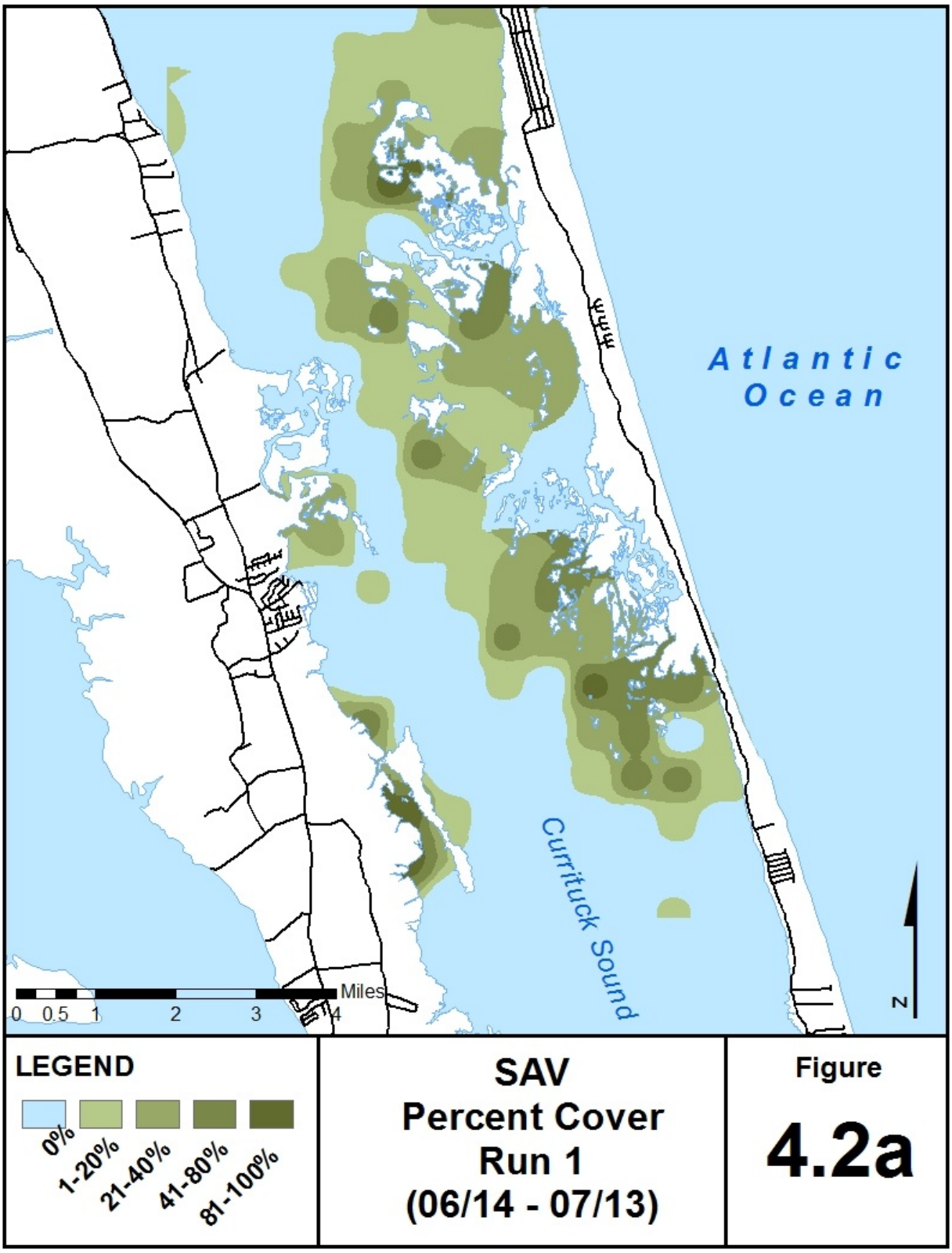

Figure 4.2a. SAV percent coverage for run 1.

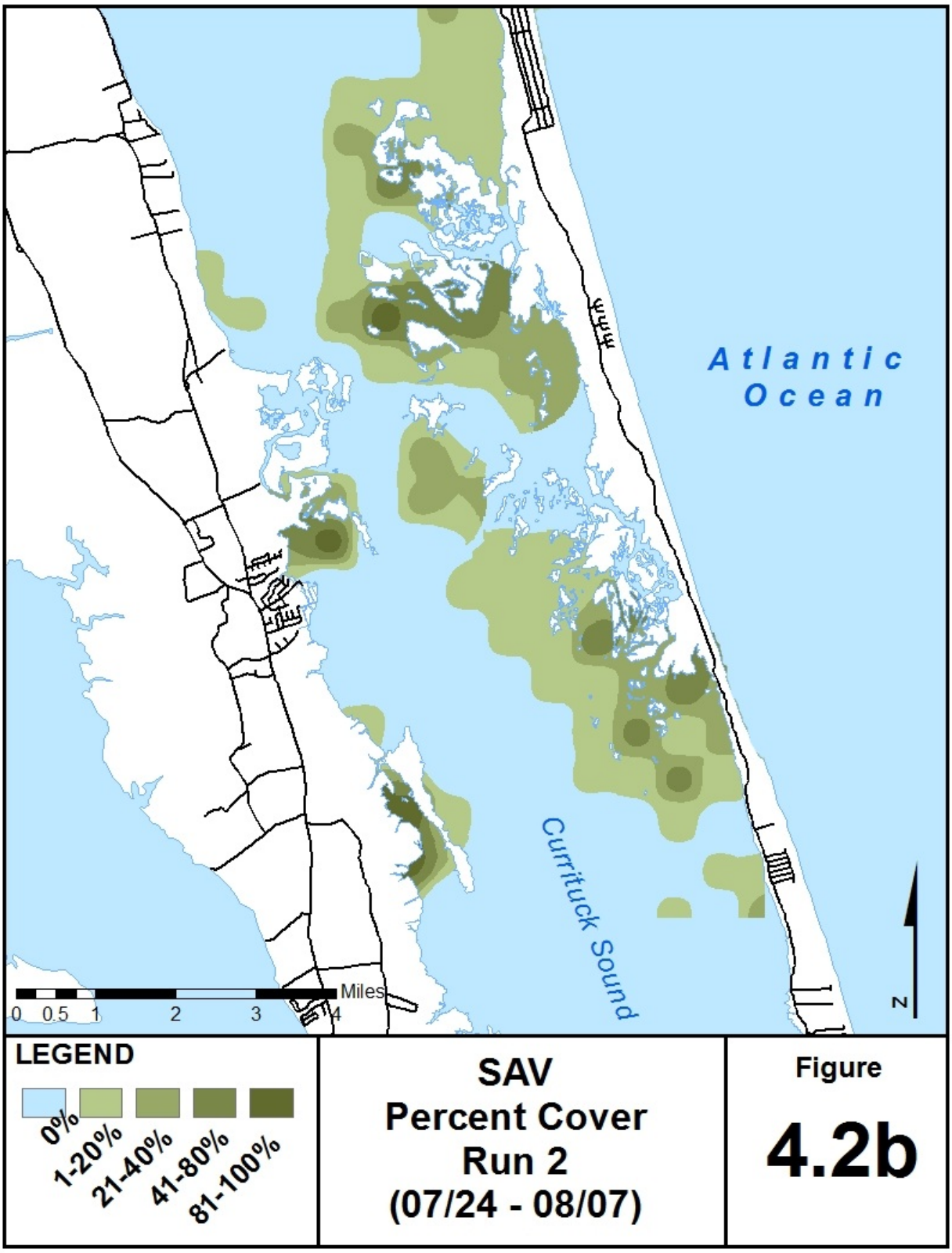

Figure 4.2a. SAV percent coverage for run 2.

4.2. SAV by Species

Six species were identified during summer sampling 2010. They were native Ruppia maritima (Widgeon grass), Najas guadalupensis (southern naiad), Stuckenia pectinata (Sago pondweed), Vallisneria americana (Eel grass), Potamogeton perfoliatus (Redhead grass) and a single invasive species , Myriophyllum spicatum (Eurasian watermilfoil). All of the six identified SAV species have been previously identified in the Currituck Sound (Sincock et al 1965). Of points with SAV present, Ruppia maritima was most widely distributed at 87% of vegetated points, followed by Stuckenia pectinata at 61% of points, Najas guadalupensis at 43% of points, Myriophyllum spicatum at 35% of points, Potomogeton at 6% of points and Vallisneria americana at 5% of points. The estimated extent of each species is presented in figures 4.3a-b, 4.4a-b, 4.5a-b, 4.6a-b, 4.7a.-b, 4.8a-b as well as the p-value for the associated Moran's-I measure of spatial autocorrelation.

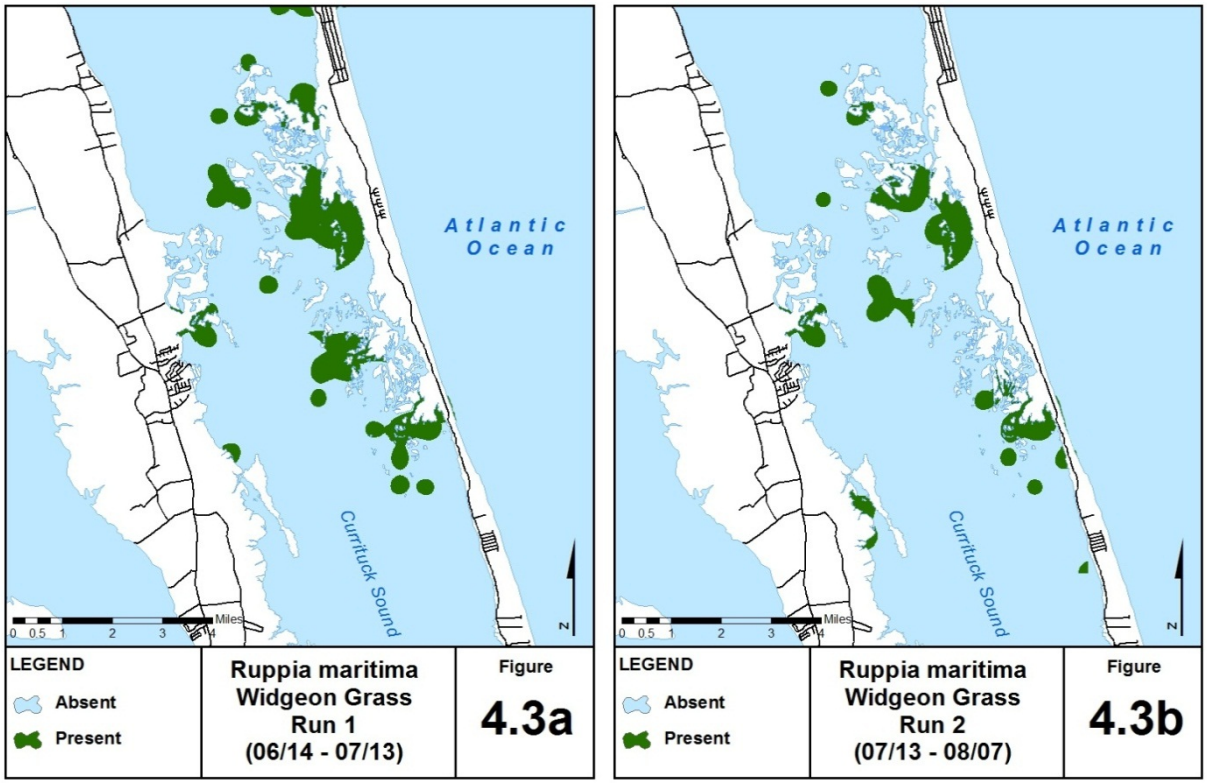

Figure 4.3 a.) Widgeon grass presence or absence for run 1 (p-value = 0.01) and **b.)** run 2 (p-value = 0.01)

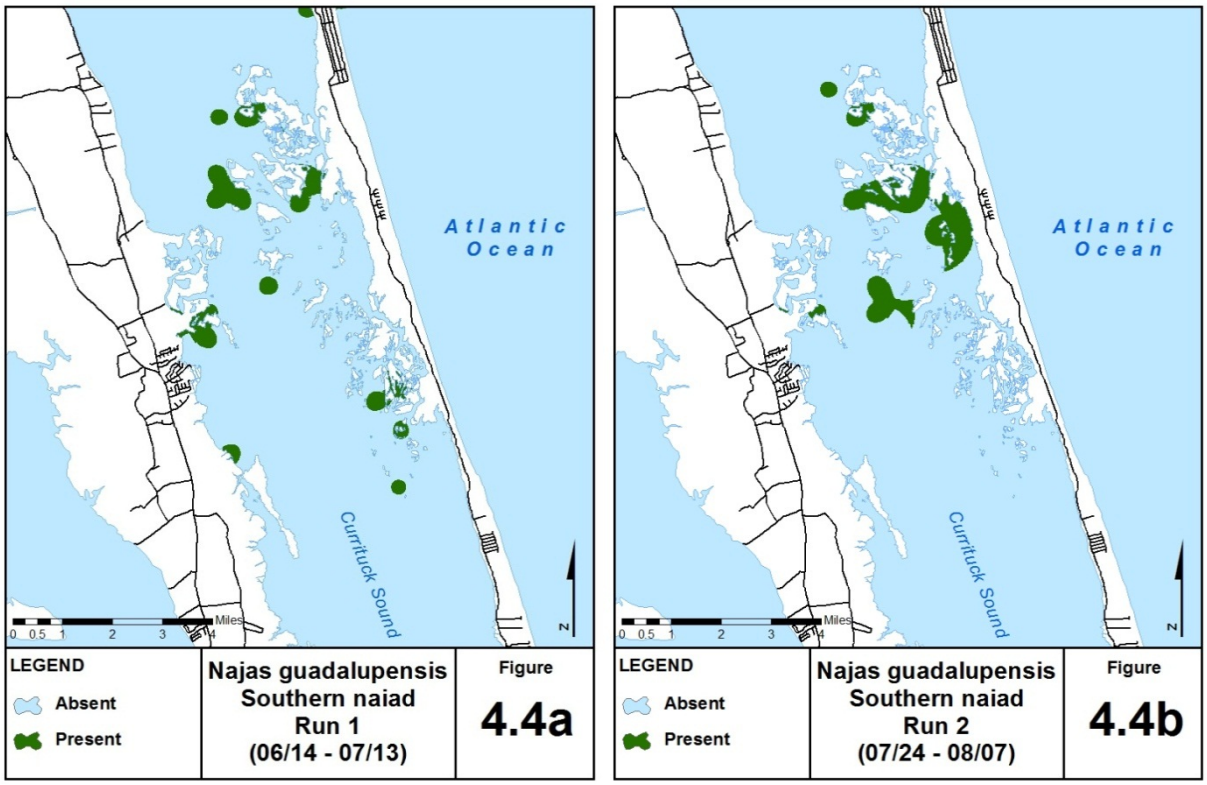

Figure 4.4 a.) Southern naiad presence or absence for run 1 (p-value = <0.001) and **b.)** run 2 (p-value = 0.01)

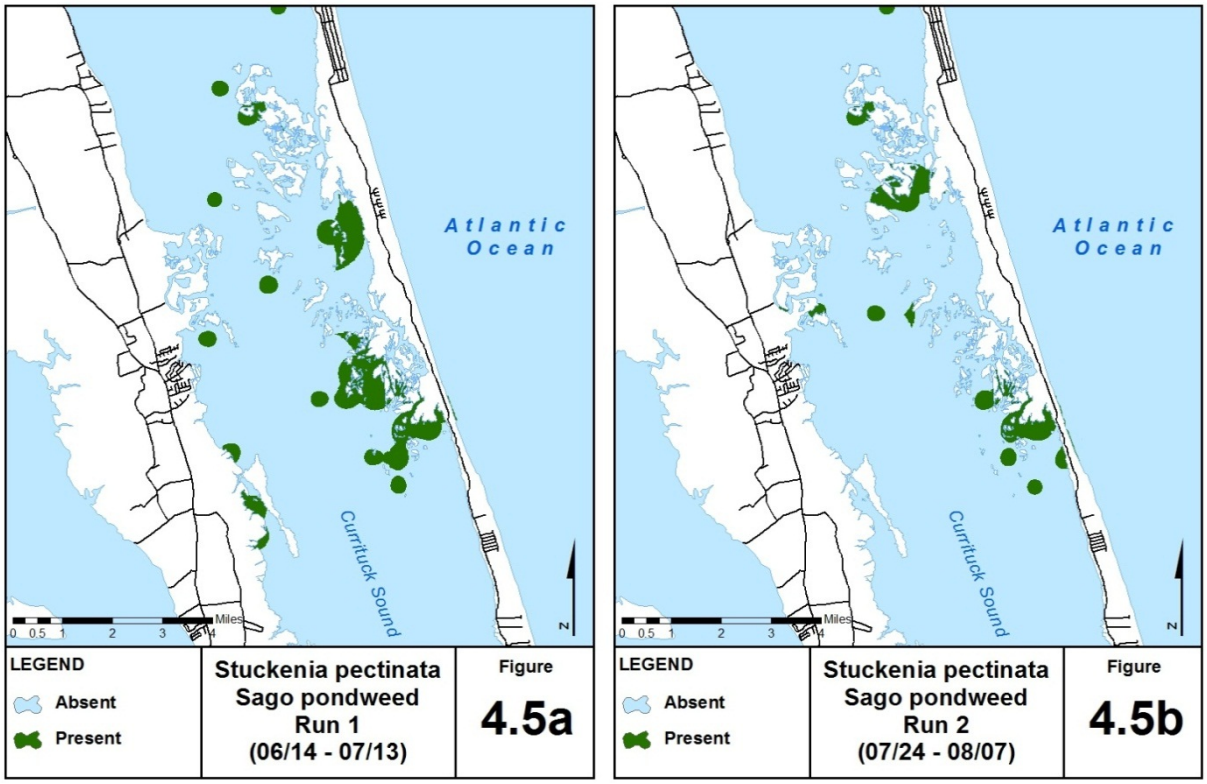

Figure 4.5 a.) Sago pondweed presence or absence for run 1 (p-value = 0.03) and **b.)** run 2 (p-value = 0.01)

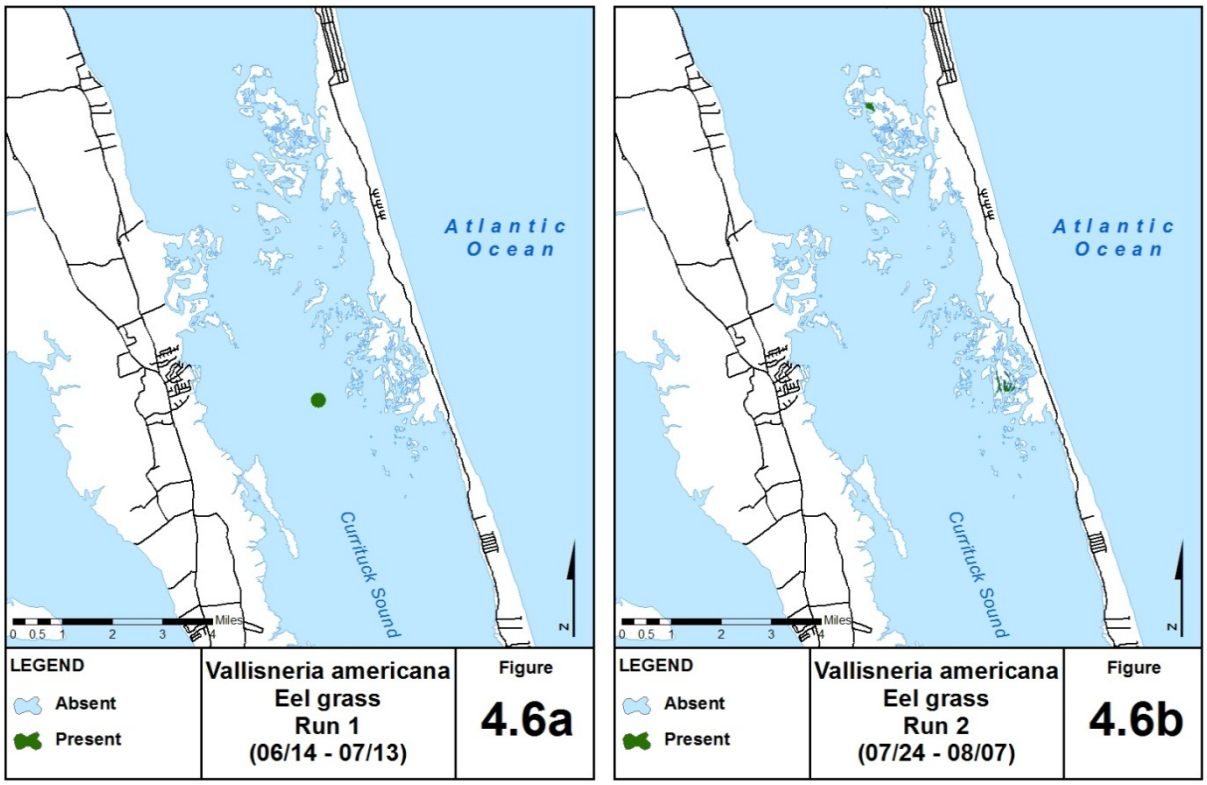

Figure 4.6 a.) Eel grass presence or absence for run 1 (p-value = n/a) and **b.)** run 2 (p-value = n/a)

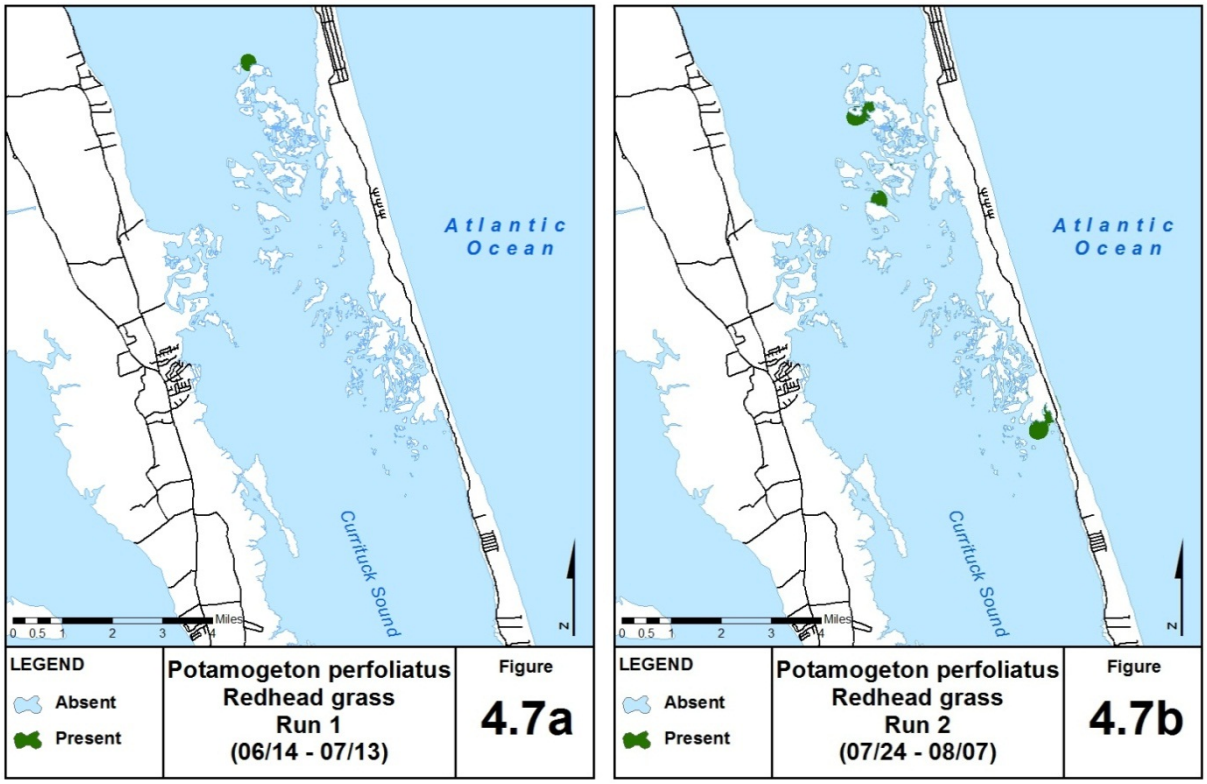

Figure 4.7 a.) Redhead grass presence or absence for run 1 (p-value = n/a) and **b.)** run 2 (p-value = 0.01)

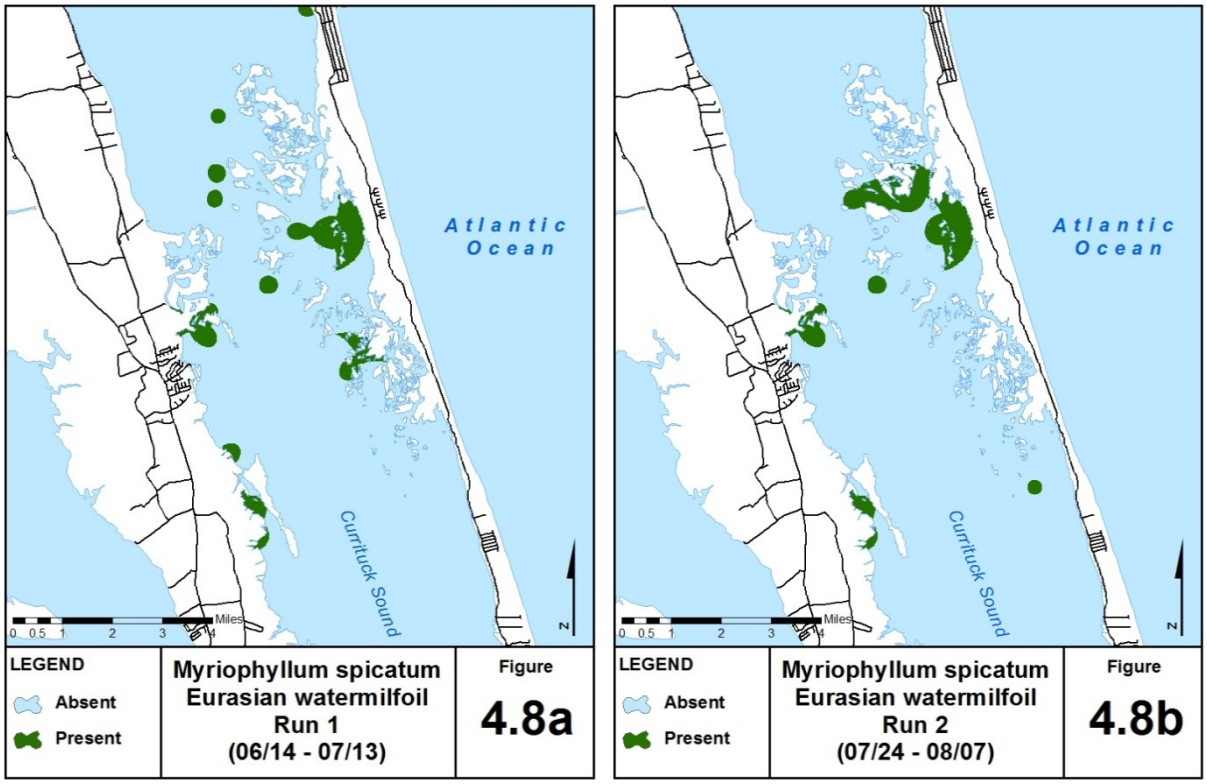

Figure 4.8 a.) Eurasian watermilfoil presence or absence for run 1 (p-value = 0.10) and **b.)** run 2 (p-value = 0.05)

Within vegetated areas, a dominant species may be present or SAV species may be intermixed. The majority of areas in Currituck Sound were found to have heterogeneous or intermixed beds of SAV with few solely homogenous beds. Therefore, species dominance was established to represent the dominant species at each point. Complete dominance is defined as an individual species representing more than 90% of a given area as determined during field sampling. Shared dominance is defined as representing as much as 50% of a given area along with one or more species. Lastly, subdominance is defined as representing less than 20% of an area however, being present in as little as trace amounts. On average, Ruppia maritima was the dominant species at 41% of vegetated points, followed by Stuckenia pectinata at 26% of points. Myriophyllum spicatum and Najas guadalupensis were dominant at less than 8% of points and Vallisneria Americana and Potamogeton perfoliatus were not found to be considered dominant at any point. Potential areas of species dominance are presented in figures 4.9a-b, 4.10a-b, 4.11a-b, 4.12a-b, 4.13a.-b, 4.14a-b.

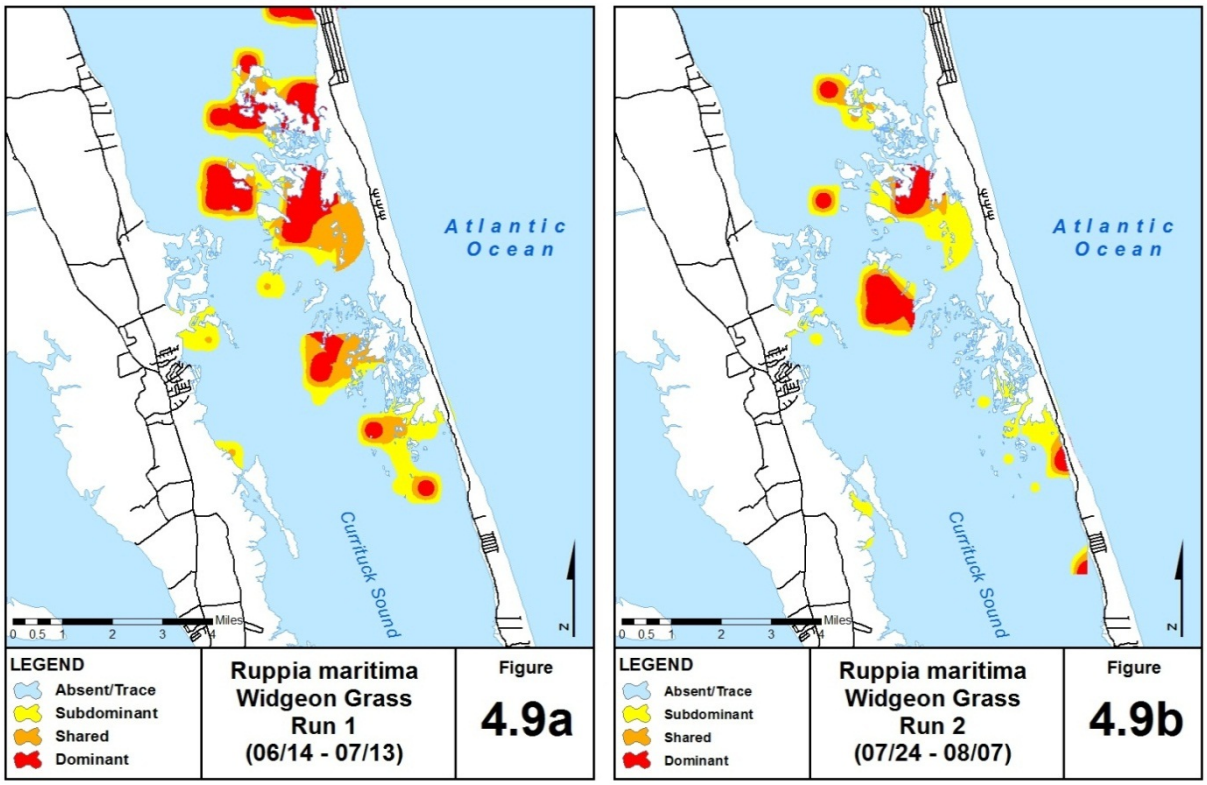

Figure 4.9 a.) Widgeon grass dominance for run 1 and **b.)** run 2

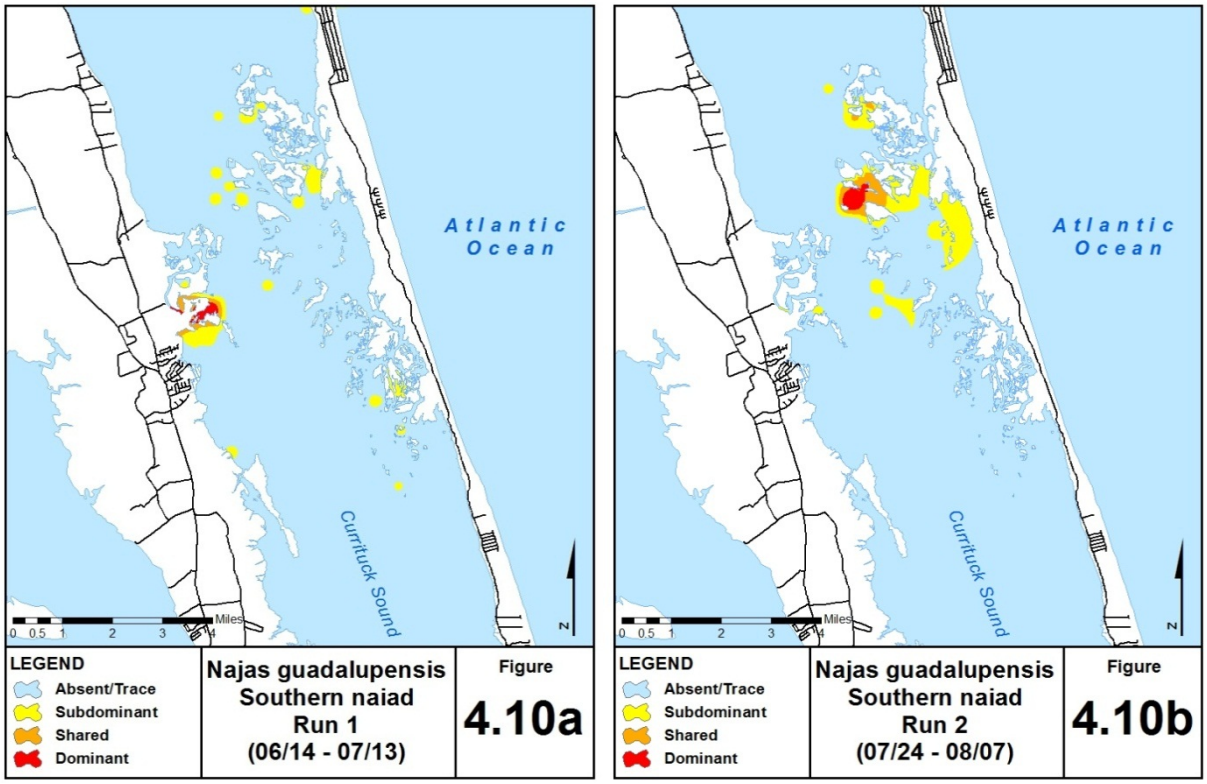

Figure 4.10 a.) Southern naiad dominance for run 1 and **b.)** run 2

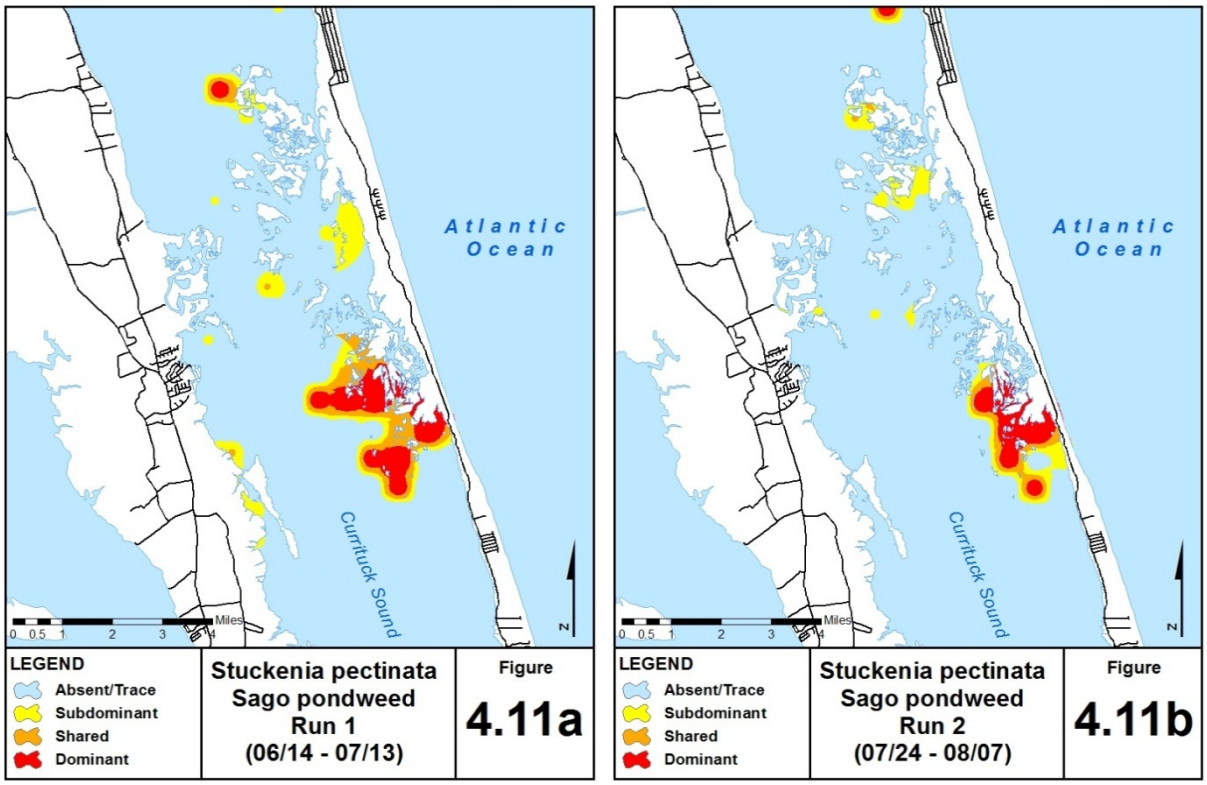

Figure 4.11 a.) Sago pondweed dominance for run 1 and **b.)** run 2

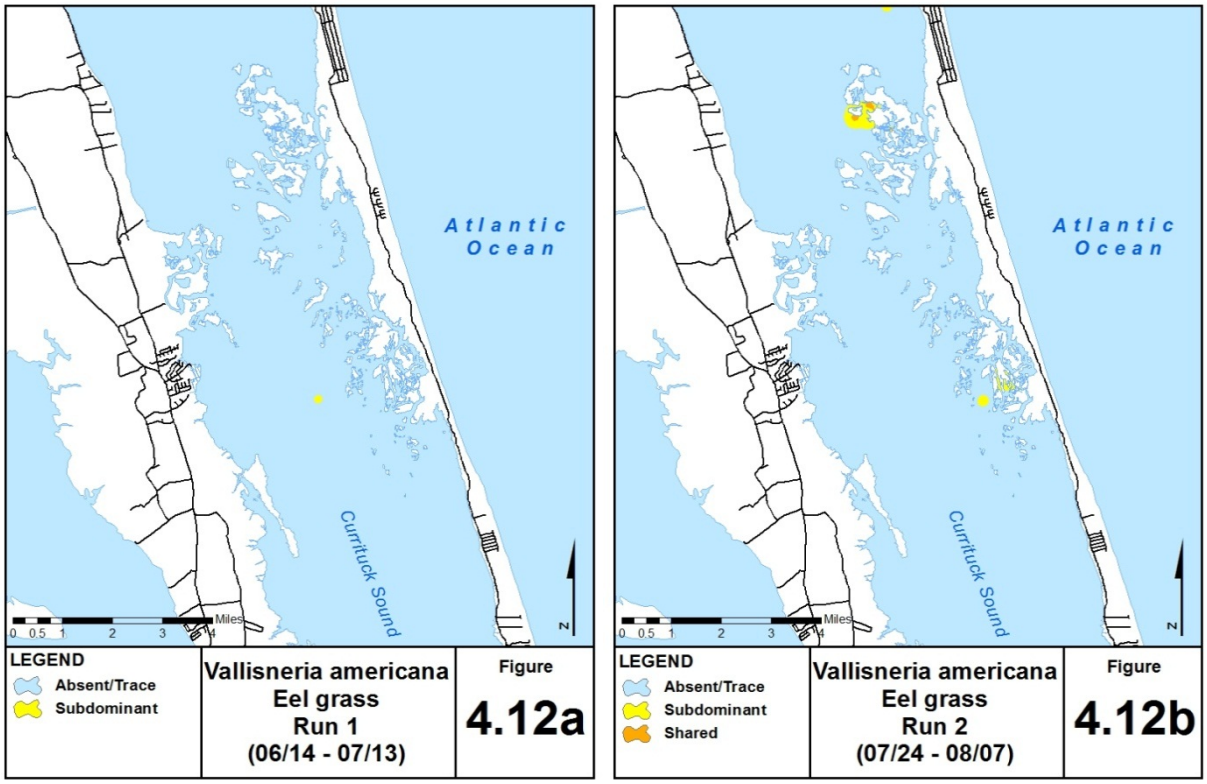

Figure 4.12 a.) Eel grass dominance for run 1 and **b.)** run 2

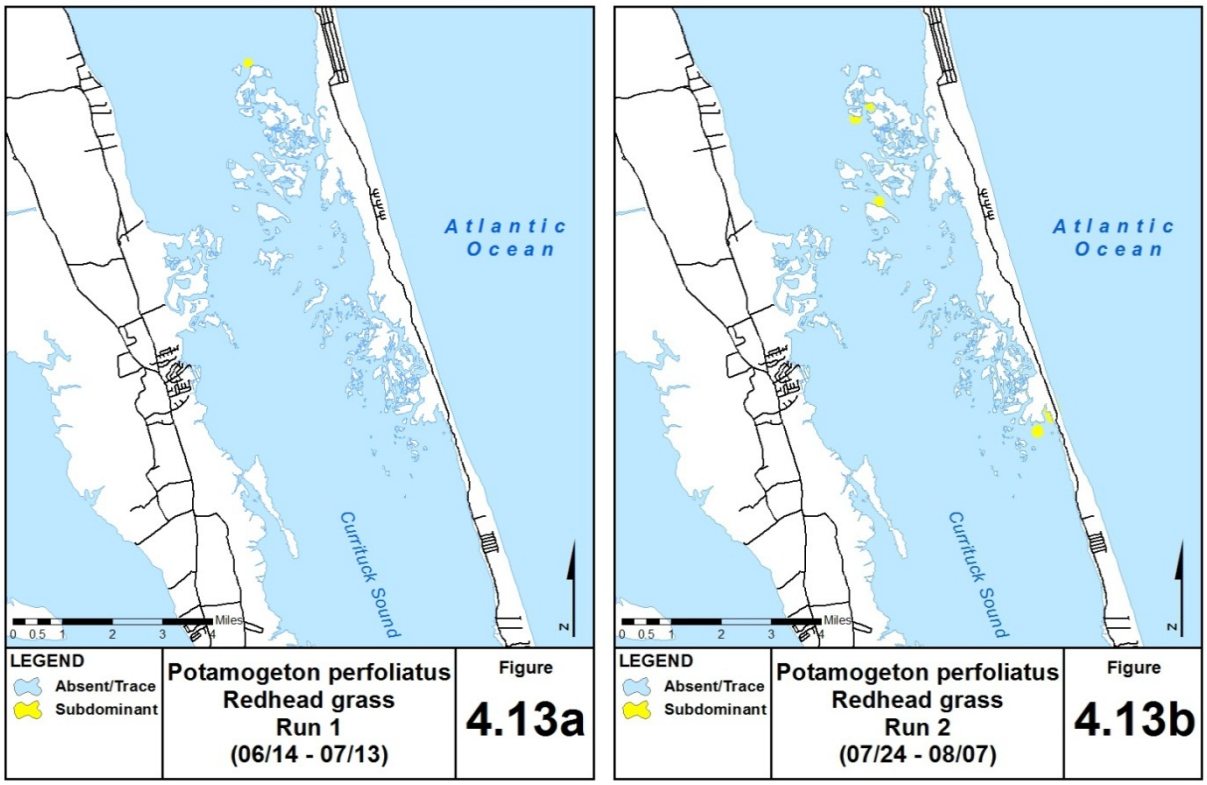

Figure 4.13 a.) Redhead grass dominance for run 1 and **b.)** run 2

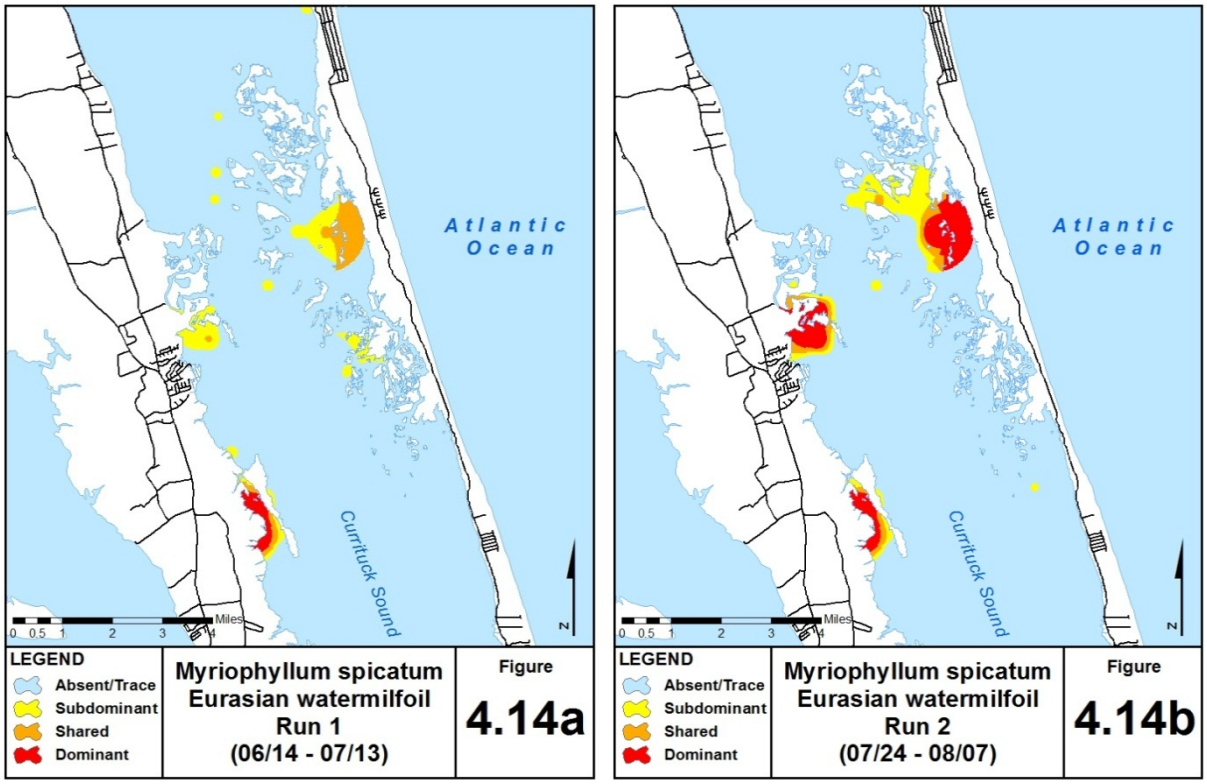

Figure 4.14 a.) Eurasian watermilfoil dominance for run 1 and **b.)** run 2

Some species were found to be highly correlated in terms of spatial distribution. Myriophyllum spicatum and Najas guadalupensis tend to be most highly correlated throughout the 2010 summer season ($p<0.0001$) whereas Ruppia maritima, and Stuckenia pectinata showed spatial correlation early in the growing season but not later (table 4.1). Species also tended to be clustered in certain areas of the Sound. Ruppia maritima, Najas guadalupensis and Stuckenia pectinata exhibited high spatial autocorrelation ($p<0.0001$) whereas Myriophyllum spicatum did not show any spatial autocorrelation with other areas of Myriophyllum spicatum (table 4.2). Vallisneria americana and Potamogeton perfoliatus could not be evaluated due to the low rate of occurrence throughout the summer.

	Species	Rumar	NaGuad	MySpic	StPect	PoPerf	VaAmer
R1	Rumar	1	**0.533** ***(0.0001)***	**0.423** ***(0.0001)***	**0.416** ***(0.0001)***	**0.197** ***(0.0324)***	0.113 *(0.2236)*
	Naguad	**0.533** ***(0.0001)***	1	0.487 ***(0.0001)***	**0.340** ***(0.0002)***	**0.185** ***(0.0453)***	-0.047 *(0.6136)*
	MySpic	**0.423** ***(0.0001)***	**0.487** ***(0.0001)***	1	**0.311** ***(0.0006)***	0.080 *(0.3871)*	-0.039 *(0.6717)*
	StPect	**0.416** ***(0.0001)***	**0.340** ***(0.0002)***	**0.311** ***(0.0006)***	1	0.018 *(0.8432)*	0.148 *(0.111)*
	PoPerf	0.197 *(0.0324)*	0.185 *(0.0453)*	0.080 *(0.3871)*	0.018 *(0.8432)*	1	-0.015 *(0.872)*
	VaAmer	0.113 *(0.2236)*	-0.047 *(0.6136)*	-0.039 *(0.6717)*	0.148 *(0.111)*	-0.015 *(0.872)*	1
R2	Rumar	1	0.152 *(0.2761)*	0.129 *(0.3554)*	-0.106 *(0.4471)*	0.092 *(0.5114)*	-0.152 *(0.2768)*
	Naguad	0.152 *(0.2761)*	1	**0.380** ***(0.005)***	0.019 *(0.8899)*	0.182 *(0.1917)*	0.038 *(0.7867)*
	MySpic	0.129 *(0.3554)*	**0.380** ***(0.005)***	1	-0.198 *(0.1535)*	0.060 *(0.6663)*	-0.085 *(0.5431)*
	StPect	-0.106 *(0.4471)*	0.019 *(0.8899)*	-0.198 *(0.1535)*	1	0.213 *(0.1246)*	0.064 *(0.6456)*
	PoPerf	0.092 *(0.5114)*	0.182 *(0.1917)*	0.060 *(0.6663)*	0.213 *(0.1246)*	1	0.188 *(0.1758)*
	VaAmer	-0.152 *(0.2768)*	0.038 *(0.7867)*	-0.085 *(0.5431)*	0.064 *(0.6456)*	0.188 *(0.1758)*	1

Table 4.1. Correlation matrix of species for run1 and run 2. Significant relationships are in bold face type.

	r1				r2			
	Moran's I	**Expected**	**P**	**Sig level**	**Moran's I**	**Expected**	**P**	**Sig level**
RuMar	**0.253235**	**-0.008621**	**0**	**0.01**	**0.268975**	**-0.008621**	**0**	**0.01**
MySpic	0.079896	-0.008621	0.053	0.1	**0.081858**	**-0.008621**	**0.0488**	**0.05**
NaGuad	**0.162014**	**-0.008621**	**0.000212**	**0.01**	**0.232964**	**-0.008621**	**0**	**0.01**
StPect	**0.091526**	**-0.008621**	**0.0306**	**0.05**	**0.4127**	**-0.008621**	**0**	**0.01**
PoPerf	n/a	n/a	n/a	(--)	n/a	n/a	n/a	(--)
VaAmer	n/a	n/a	n/a	(--)	n/a	n/a	n/a	(--)

Table 4.2. Spatial Autocorrelation of each species for run1 and run 2. Significant relationships are in bold face type.

4.3. Other Variables of Interest

4.3.1. Depth

The mean depth of the sound during sampling was 5.69 feet (1.97 SD) with a minimum depth of 1.1 feet and a maximum depth of 10.5 feet. It was estimated that greater than 50% (53.80%) of all points sampled were within the littoral zone (< 6 ft). The littoral zone depth profile was mapped using an IDW approach and is presented in figure 4.15. The mean depth containing SAV was 3.98 feet which differed significantly from the mean depth at which SAV was not present (6.40 feet). Species tended to vary little by depth with Vallisneria americana and potamogeton perfoliatus preferring somewhat shallower depths (3-3.5 ft) as compared to invasive Myriophyllum spicatum inhabiting deeper waters (4.5-6ft).

Figure 4.15. Littoral zone depth profile (feet) as estimated using points from SAV sampling summer 2010.

4.3.2. Secchi Depth

The mean secchi depth during sampling was 0.46 meters (0.1222 SD) with a minimum secchi depth of 0.2 meters and a maximum secchi depth of 0.75 meters. The mean secchi depth at which SAV was present was 0.44 meters (0.1222 SD) but did not differ from the average secchi depth of samples with no SAV present. The average secchi depth throughout sampling can be viewed in figure 4.16.

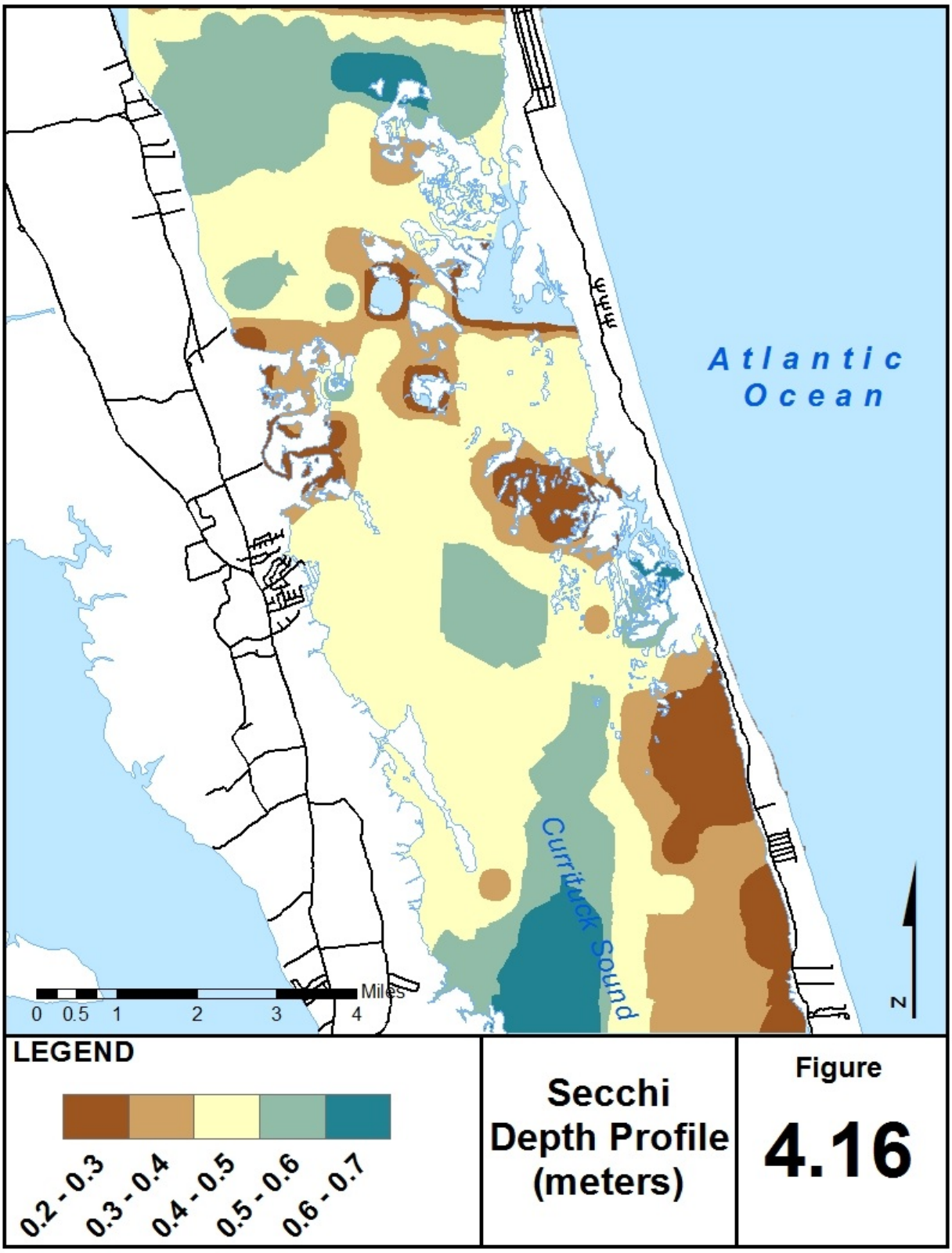

Figure 4.16. Example of secchi depth distribution as estimated using SAV sampling run 1.

4.3.3. Salinity

Salinity values seemed to vary from one sample run to the next suggesting potential surges of saline water throughout the summer growing period. Initial sampling yielded an average salinity value of 0.79 ppt ranging from 0 ppm to 6.0 ppt. During the second run of sampling, there was an overall spike of salinity to an average of 2.733 ppt with a minimum of 0.35 ppm to a maximum of 6.0 ppt. During the first run, SAV were found to be present at a mean salinity of 0.41 ppt (0.64 SD) in a range from 0 to 2.5 ppt. This differed significantly from Sampled points with no SAV which had a mean salinity of 1.04 ppt and ranged from 0 to 6 ppt. The second run yielded opposite results to salinity as levels were actually higher on average at sample points containing SAV (3.11 ppt, 1.15 SD) than at sample points with no SAV (2.64 ppt, 0.97 SD). Sampled points with and without SAV ranged from 0 to 6 ppt. Estimated salinity distribution throughout the sound during summer 2010 are displayed in figures 4.17 a and b.

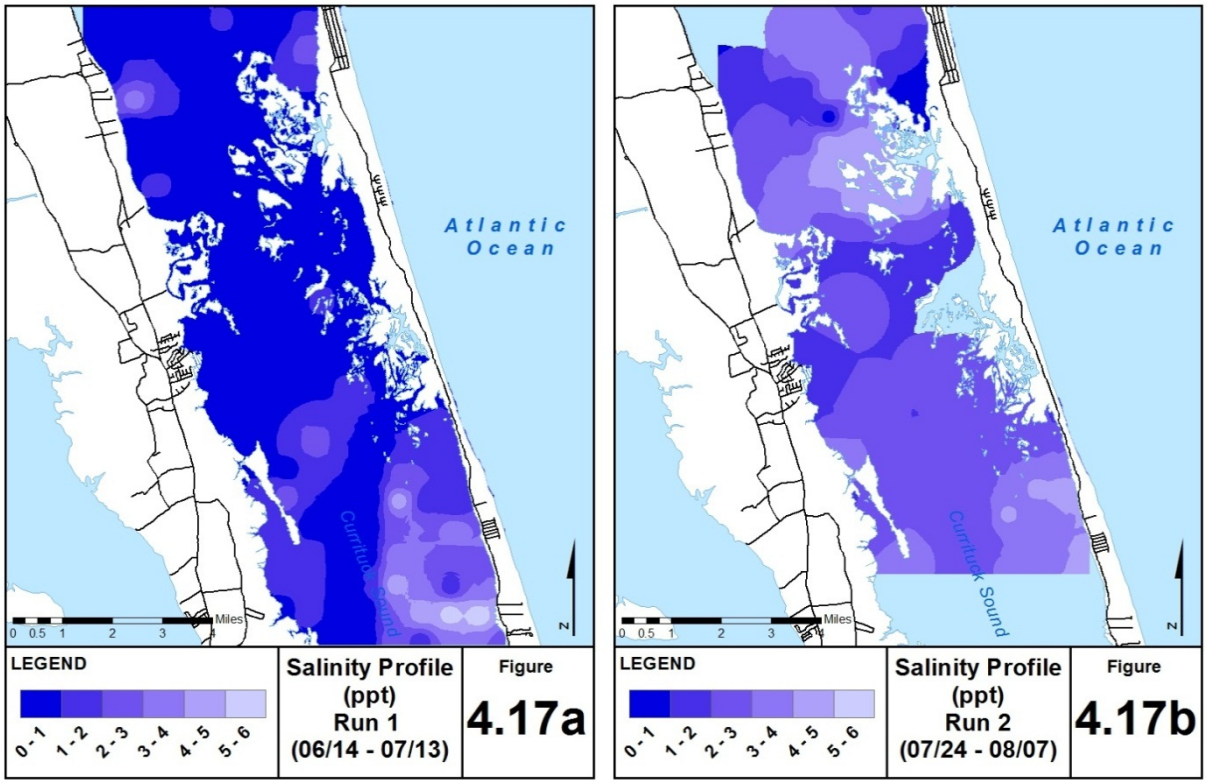

Figure 4.17 a.) Estimated salinity distribution for run 1 and **b.)** run 2

4.3.4. Water Temperature

Water temperature showed very little variation from the start of sampling until completion. Water temperature on average was around 84 degrees Fahrenheit ranging from 72 to 90 degrees Fahrenheit. Temperature did not show any significant effect in whether SAV was present or absent in a given area.

4.3.5. Sediment Type

Sediment types were identified and classified into ten categories. These are clay, clay loam, loam, loamy sand, sand, sandy clay loam, sandy loam, silt, silt clay and silt loam. The sampled areas were primarily made up of Sand (22.22%), Loamy Sand (21.05%) or Loam (19.88%). Sediment type distribution can be seen in figure 4.18. Because SAV presence/absence shows a strong relationship with depth, sediment types for vegetated areas in the littoral zone were analyzed to see if soil preference was present. The Littoral zone (< 6 feet or 1.83 meters) was made up mostly of Sand (27.17%). Sediment type distributions for the littoral zone are presented in table 4.3. Vegetated areas in the littoral zone seemed to show little preference for any one sediment type, however SAVs were most often not found in areas with a sediment type of sand. Distributions of vegetated points by sediment type are presented in figure x.

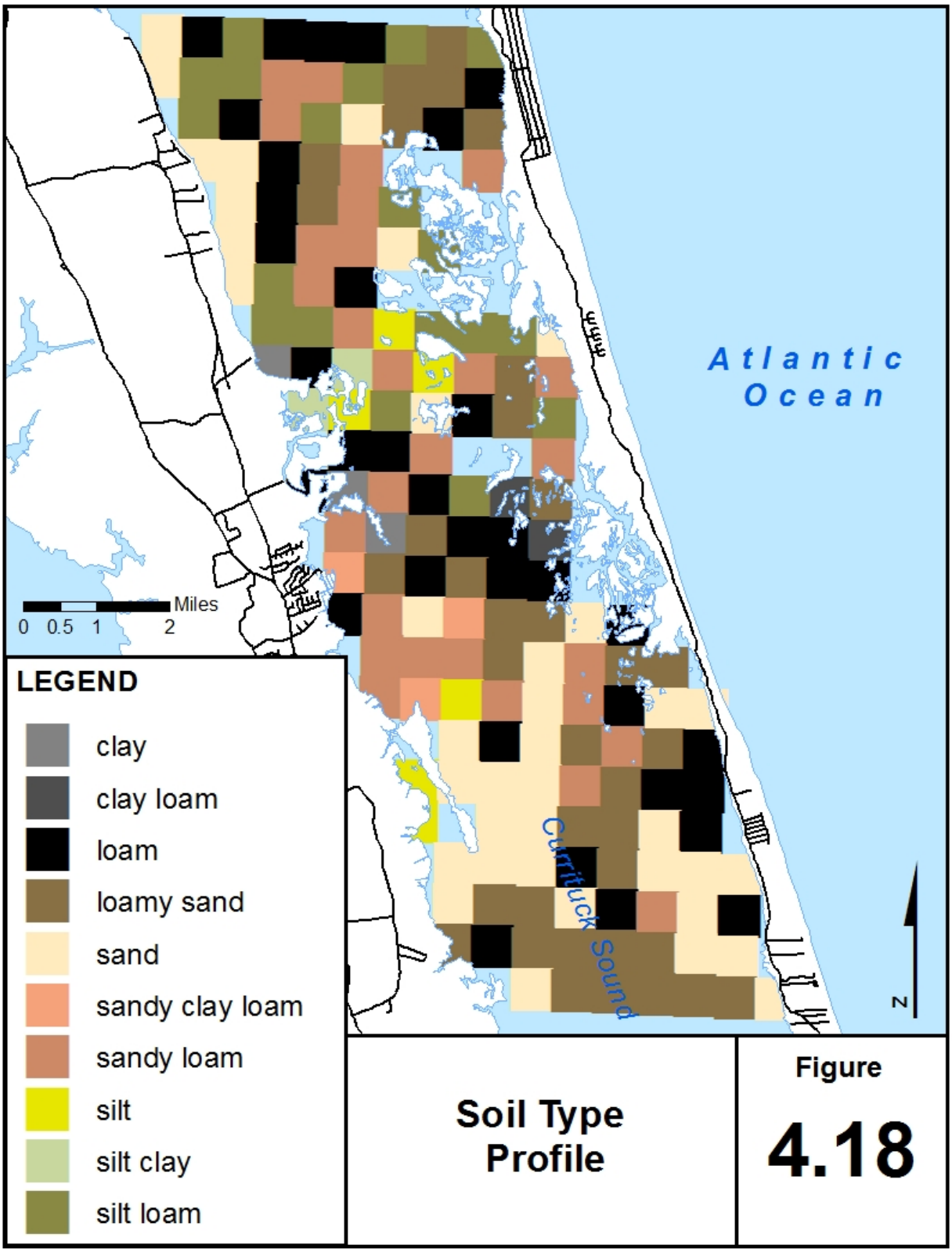

Figure 4.18. Distribution of soil type throughout the study area as estimated during SAV sampling of summer 2010.

Sediment Type	Frequency	Percent	Vegetated	Percent Vegetated
clay	1	1.09	1	100%
clay loam	2	2.17	1	50.00%
loam	13	14.13	7	53.85%
loamy sand	19	20.65	11	57.89%
sand	25	27.17	2	8.00%
sandy clay loam	2	2.17	0	0.00%
sandy loam	17	18.48	13	76.47%
silt	3	3.26	2	66.67%
silt clay	1	1.09	0	0.00%
silt loam	9	9.78	5	55.56%

Table 4.3. Sediment type distribution of the littoral zone and number of vegetated points in each.

4.4. SAV Change

The Sincock reports were a series of reports made available in 1965 and 1966 as a cooperative effort to identify the primary physical, chemical and biological factors responsible for the reduction in wildlife and fish use of the Currituck Sound, NC and Back Bay, VA. The data were compiled into four volumes (Introduction and Vegetation Studies, Waterfowl Studies, Fish Studies, and Environmental Factors) in a cooperative effort between the Bureau of Sport Fisheries and Wildlife, North Carolina Wildlife Resources Commission and the Virginia Commission of Game and Inland Fisheries (Sincock et al 1965). This study is the last known extensive SAV sampling program to have taken place on the Currituck Sound until present day. Estimations of SAV presence and absence are comparable among the Sincock Reports findings (transects N-R: Sincock et al 1965) and the study area used during this study. An overall decrease in SAV presence of 31.53% was estimated between the last known sampling of the entire area (1964) and present day from 77.20% SAV presence in 1964 to 45.67% SAV presence as of 2010. See figure 4.19.

The Currituck Sound has also seen a shift in species evenness when compared to the Sincock data (1958-1962). The dominant species during the Sincock reports was Najas guadalupensis (50.60%) with equal representation of Ruppia maritima, Stuckenia pectinata, Potamogeton perfoliatus and Vallisneria americana, each between 20 and 30% of all points sampled. The 2010 survey suggests Ruppia maritima as the dominant species (40.60%) with Najas guadalupensis and Stuckenia pectinata representing between 20% and 30% of all points sampled. Potamogeton perfoliatus and Vallisneria americana are reduced to presence of only 2 to 3% of all points sampled, only 10% of the Sincock estimates. The 2010 survey also shows a 17% representation of Myriophyllum spicatum, an invasive plant thought to have been introduced in the late 1960s which was not present during the time of the Sincock reports. See

figure 4.20 for a graphical representation of species present during the Sincock reports (4.20a) and of the present study (4.20b).

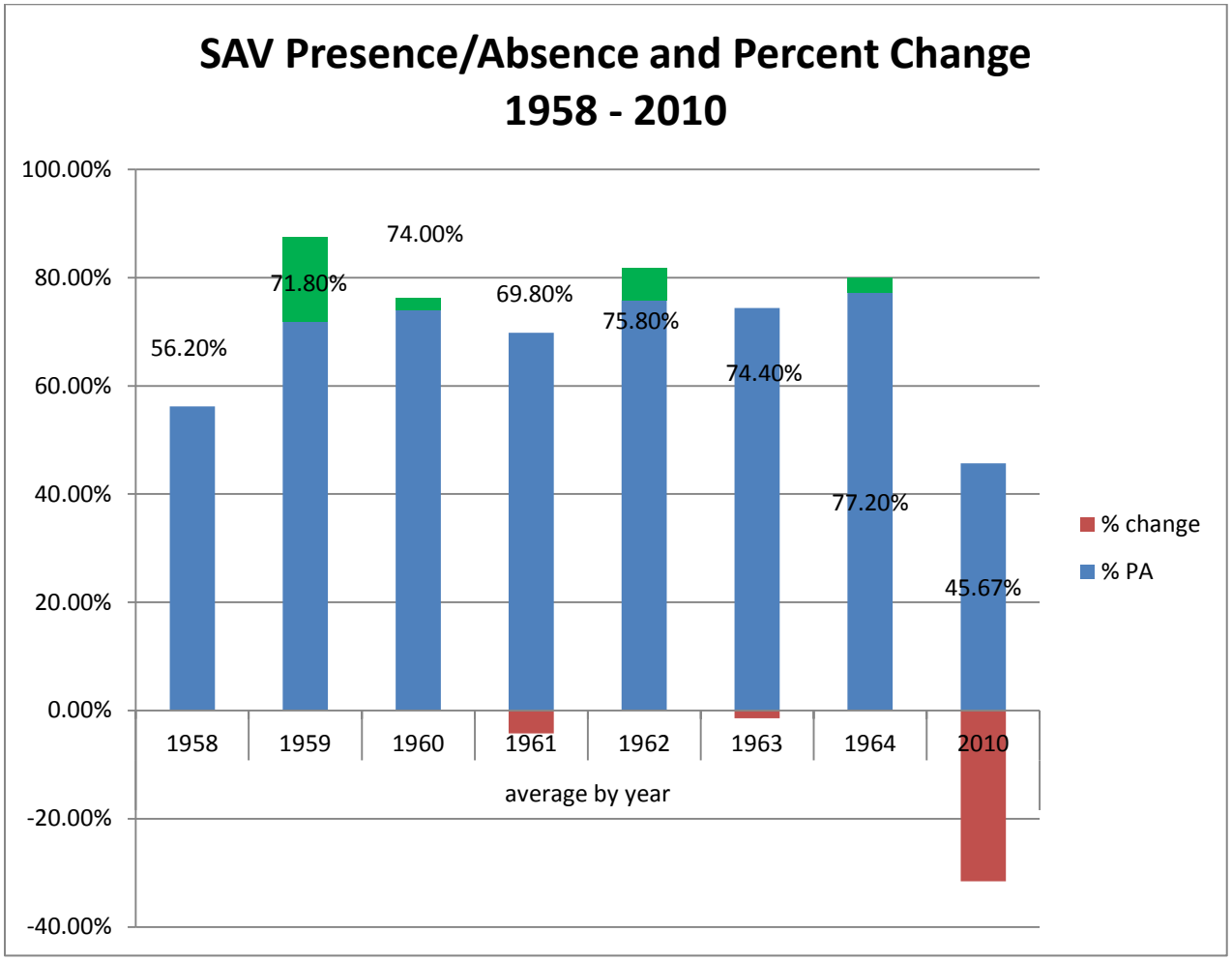

Figure 4.19. SAV presence/absence percent change estimated using Sincock reports and current study.

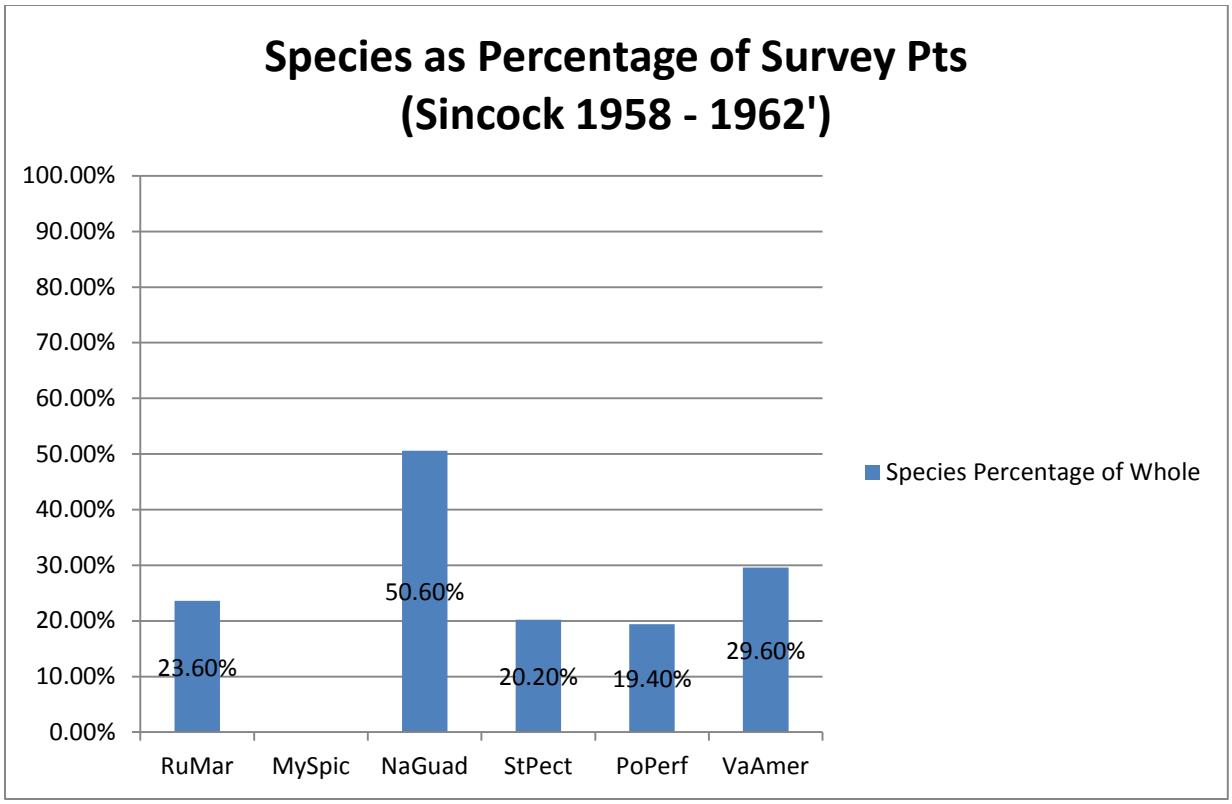

Figure 4.20 a.) Species as a percentage of all vegetated points as estimated using the Sincock reports.

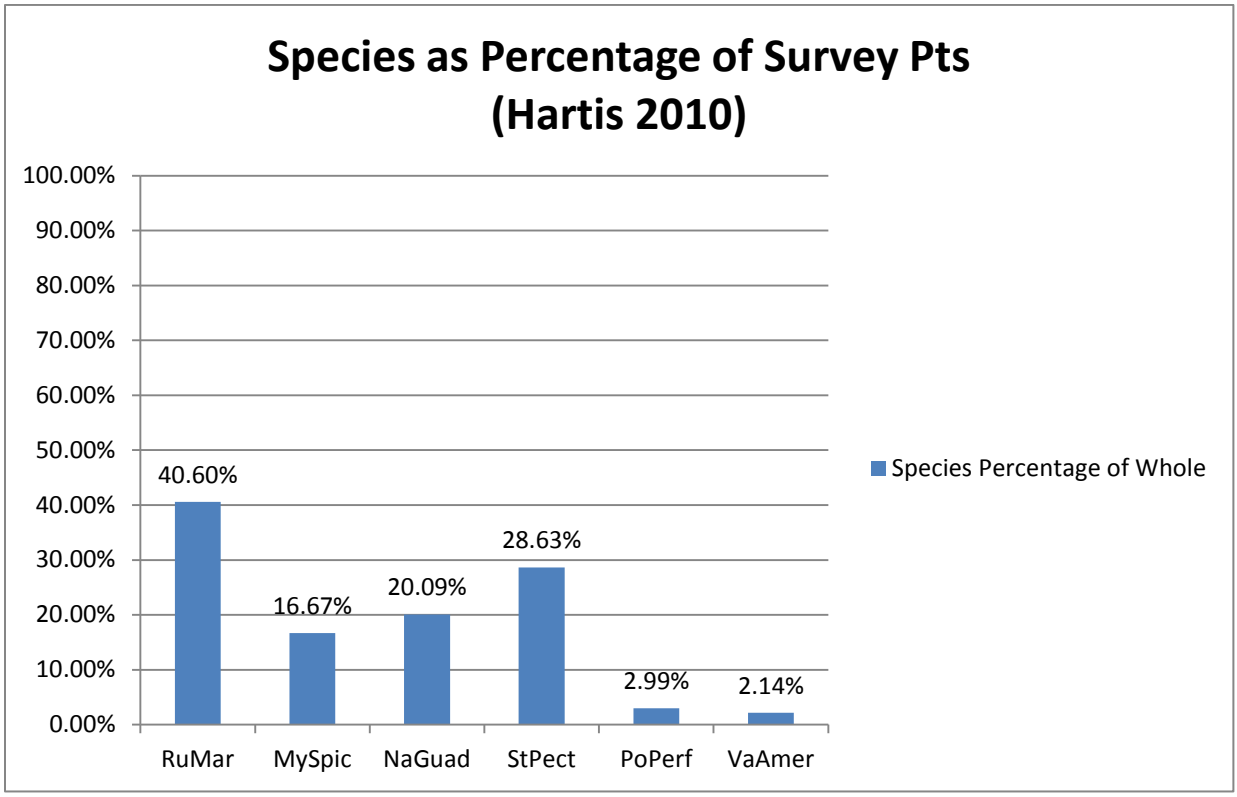

Figure 4.20 b.) Species as a percentage of all vegetated points as estimated in the summer 2010 study.

4.5. LOGIT Model Results

Sensor specific models proved to be the best approach for predicting SAV presence or absence. No models could be developed for the multinomial variable (plant cover) due to a low ratio of events to non-events. In the case of the multinomial variable (plant cover), an event is defined as any plant cover category 1-3 which indicated some type of SAV presence. A non-event is defined as the plant cover category 0 which indicated no plant presence. One of the automated selection methods (i.e. forward, backward, best subset, and/or stepwise) produced the final models we selected for each sensor. The automated best-subsets method allowed for exploration of a number of potential candidate models based on the number of variables input in the model. The automated stepwise selection method led to the final, most reasonable model as decided upon in the best-subset procedure. For a variable to enter into or remain in the model, a p-value of <0.01 was necessary. A model was considered fit if the Hosmer and Lemeshow test yielded an insignificant difference in groups ($p>0.05$). Sensor specific models were developed for both the Quickbird and Worldview-II sensors, however LANDSAT 5 specific models were inconclusive for a number of reasons. We used odds ratios to evaluate relative influence of variables selected in the final models. Prediction maps are displayed as correct prediction (prediction = observation), false positives (prediction = 1, observation = 0), or false negatives (prediction = 0, observation = 1). False negatives are thought to be a product of depth whereas false positives could be a product of contributions from sources other than SAVs. Differences between sensor models might be attributed to variation in band width across each sensor. A number of difficulties occurred during model development for both the binomial variable (presence/absence) and the multinomial variable (plant cover category). Efforts to develop multinomial variable models were unsuccessful due to a low occurrence of events to nonevents.

4.5.1. Worldview-II

The Worldview-II sensor provided the most adequate predictive model of the binary predictor variable (presence/absence) with percent concordant values between 88.5 and 94.7% and Wald, Likelihood and Score values of <0.0001 each. Three variables were included in the Worldview-II sensor specific prediction model (table x). The most influential predictor variable for the Worldview-II sensor specific model was the interaction between band 4 and secchi depth, followed by the interaction between band 3 and secchi depth, band 4 alone and band 3 alone. The negative β coefficient for band 4 alone is consistent with knowledge of the reflective properties of submersed plants in wavelengths from 700 to 1100 nanometers. The negative β coefficient associated with the interaction of band 3 and secchi depth is consistent with both the reflective properties of plants in wavelengths from 600 to 700 nanometers and the association that light penetration decreases as secchi depth increases. The exact opposite can be said for both the positive associations with band 3 alone and the interaction between band 4 and secchi depth. In regards to the best image provided for the Worldview-II sensor (08/05/10), model outputs demonstrated only 4 false negatives (observation dataset = presence,

prediction dataset = absence) and 3 false positives (observation datatset = absence, prediction dataset = presence). False negatives and false positives were most often observed in shallow water (< 3 feet). This could suggest that depth plays a secondary role in the ability of each sensor to detect SAV at certain depths. One of the three false positives was actually located at a point with SAV coverage of 0-10%, however this point was designated for SAV absence because this did not cross the 20% or greater threshold for SAV presence. The same model applied to the lowest quality Worldview-II image (07/22/10) yielded 1 false positive and 15 false negatives. The only false positive predicted was also located at a point with SAV coverage of 10-20%, however this point was also designated for SAV absence because this did not cross the 20% or greater threshold for SAV presence. Due to the poor quality of the Worldview-II image taken on 07/22/10, an image specific model was developed for the best Worldview-II image (08/05/10) to test for any difference. The image specific model contained only two of the original three variables that were used for prediction in the Worldview-II sensor specific model. This image specific model suggested that only the interaction between band 4 and secchi depth was the best predictor for the model. This image specific model yielded a percent concordant value of between 88.5 and 94.7 and a Wald, Likelihood and Score values of <0.001. The positive β coefficient association with the interaction between band 4 and secchi depth is consistent with knowledge of the reflective properties of SAV from 700 to 1100 nanometers and was similar to that association in the sensor specific model. The image specific model yielded 3 false positives and 5 false negatives however. False positives were predicted in shallow areas (<3 feet) and false negatives were predicted in deeper water (> 3 feet). Two of the three false positives were actually located at points with SAV coverage of 10-20%, however these points were designated for SAV absence because this did not cross the 20% or greater threshold for SAV presence. Parameter estimates for each Worldview-II model can be found in tables 4.4 and 4.5 for the sensor specific model and in table 4.6 for the image specific model. All prediction outputs for the two proposed Worldview-II sensor derived models can be found in figure 4.21a (08/05/10 dataset), 4.22 a (07/22/10 dataset), as well as for the image specific model (08/05/10 dataset) in 4.23a. For comparison of prediction output to actual ground truth estimations, SAV percent cover is overlain for each image/model combination in figures 4.21 b (08/05/10 dataset), 4.22b (07/22/10 dataset) and the image specific model in 4.23b (08/05/10 dataset).

Analysis of Maximum Likelihood Estimates					
Parameter	DF	Estimate	Standard Error	Wald Chi-Square	Pr > ChiSq
Intercept	1	-2.2755	0.7678	8.7843	0.003
B3	1	0.5497	2.1038	0.0683	0.7939
B4	1	-4.9392	3.0326	2.6527	0.1034
B3*SD	1	-5.4005	4.6811	1.3309	0.2486
B4*SD	1	21.6477	9.0837	5.6793	0.0172

Table 4.4. Parameter estimates for the Worldview-II sensor specific model applied to the 08/05/10 dataset.

Analysis of Maximum Likelihood Estimates					
Parameter	DF	Estimate	Standard Error	Wald Chi-Square	Pr > ChiSq
Intercept	1	-1.8425	0.295	39.0086	<.0001
B3	1	19.1947	7.5488	6.4655	0.011
B4	1	-22.3063	7.8728	8.0278	0.0046
B3*SD	1	-46.3251	20.0271	5.3506	0.0207
B4*SD	1	53.8189	20.6317	6.8045	0.0091

Table 4.5. Parameter estimates for the Worldview-II sensor specific model applied to the 07/22/10 dataset.

Analysis of Maximum Likelihood Estimates					
Parameter	DF	Estimate	Standard Error	Wald Chi-Square	Pr > ChiSq
Intercept	1	-2	0.4859	16.94	<.0001
B4*SD	1	5.8799	1.3345	19.4146	<.0001

Table 4.6. Parameter estimates for the best Worldview-II image specific model applied to the 08/05/10 dataset.

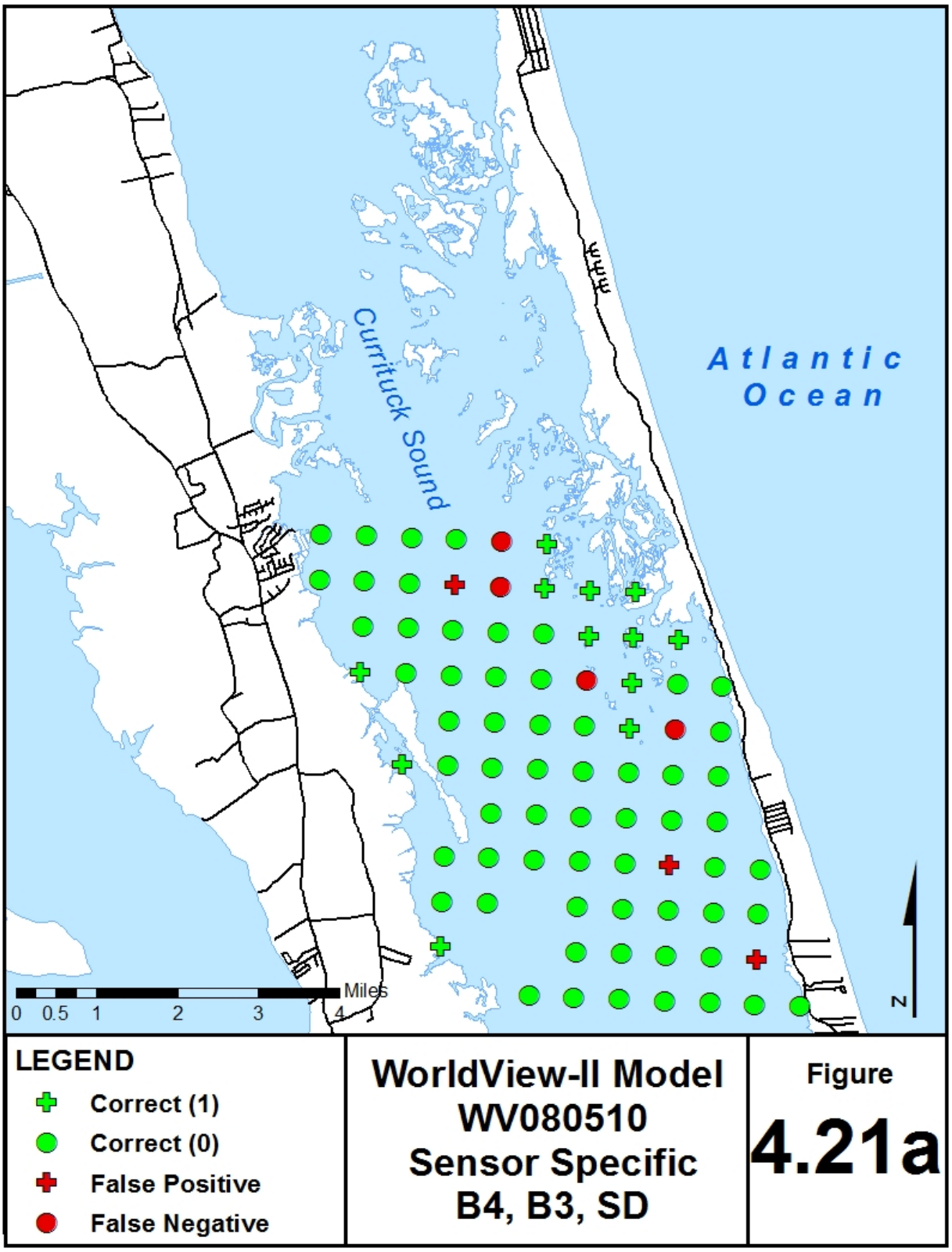

Figure 4.21a. Worldview-II sensor specific model applied to image taken on 08/05/10.

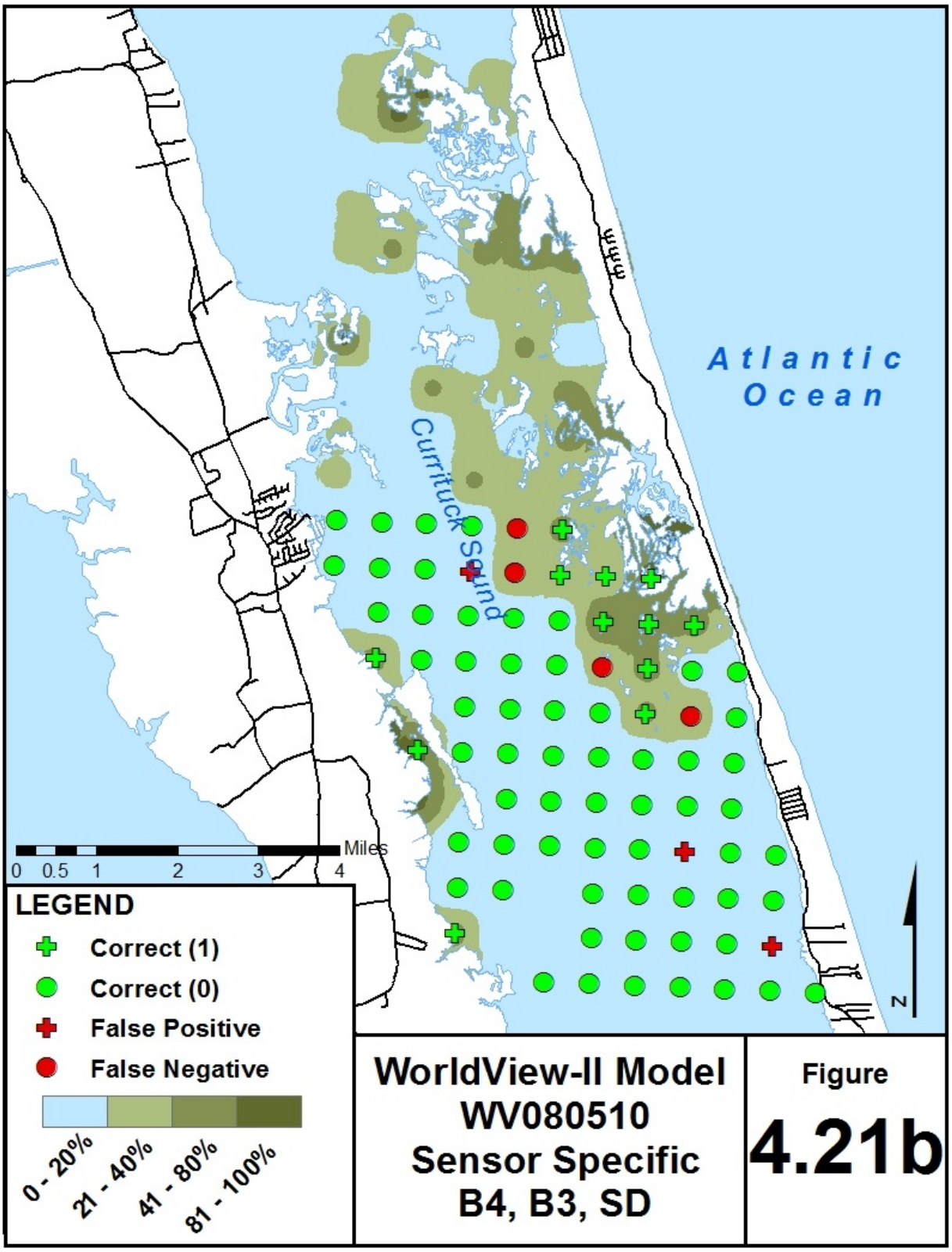

Figure 4.21b. Worldview-II sensor specific model predictions applied to image taken on 08/05/10 and overlain with SAV percent cover estimations from ground truthing run 2.

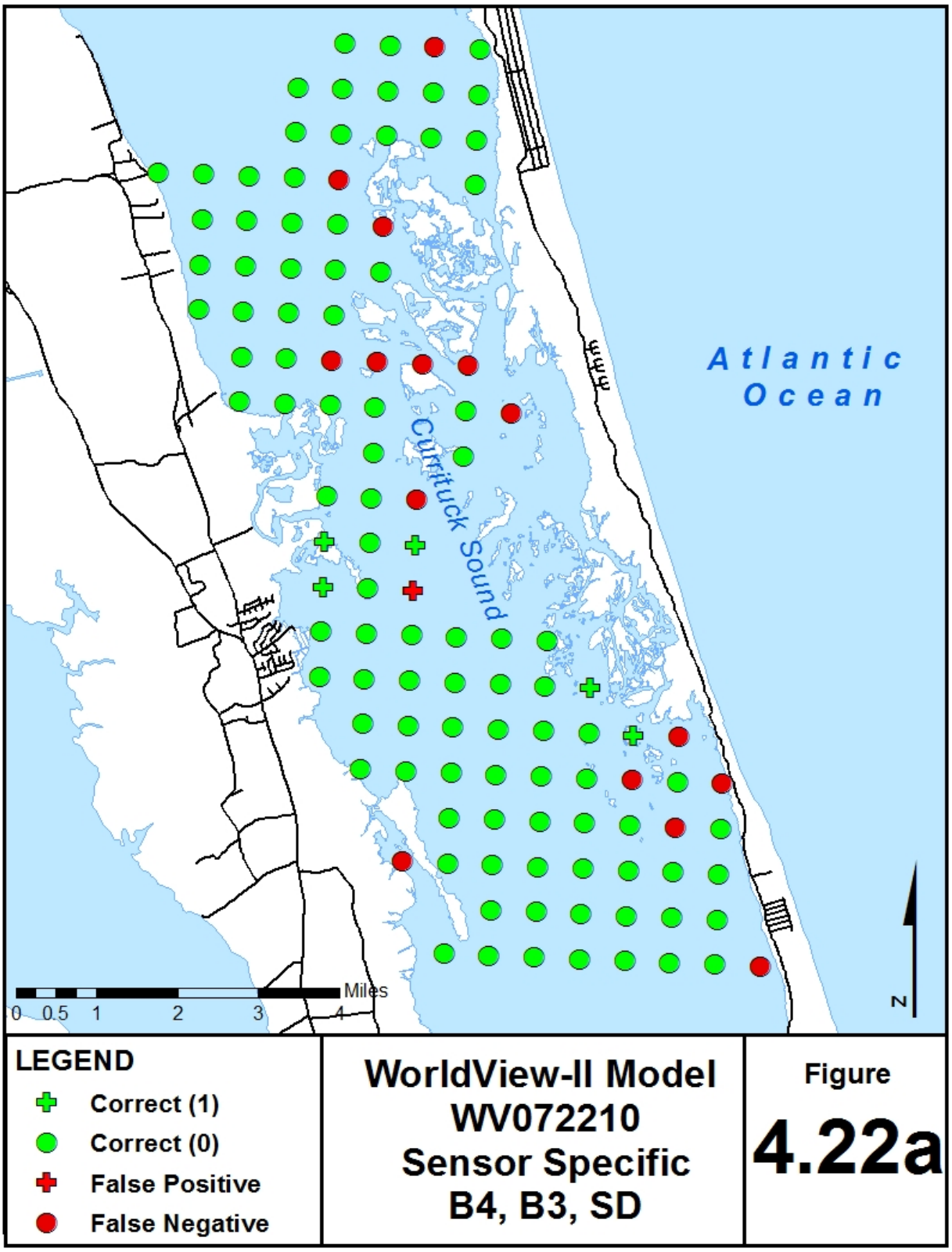

Figure 4.22a. Worldview-II sensor specific model predictions applied to image taken on 07/22/10.

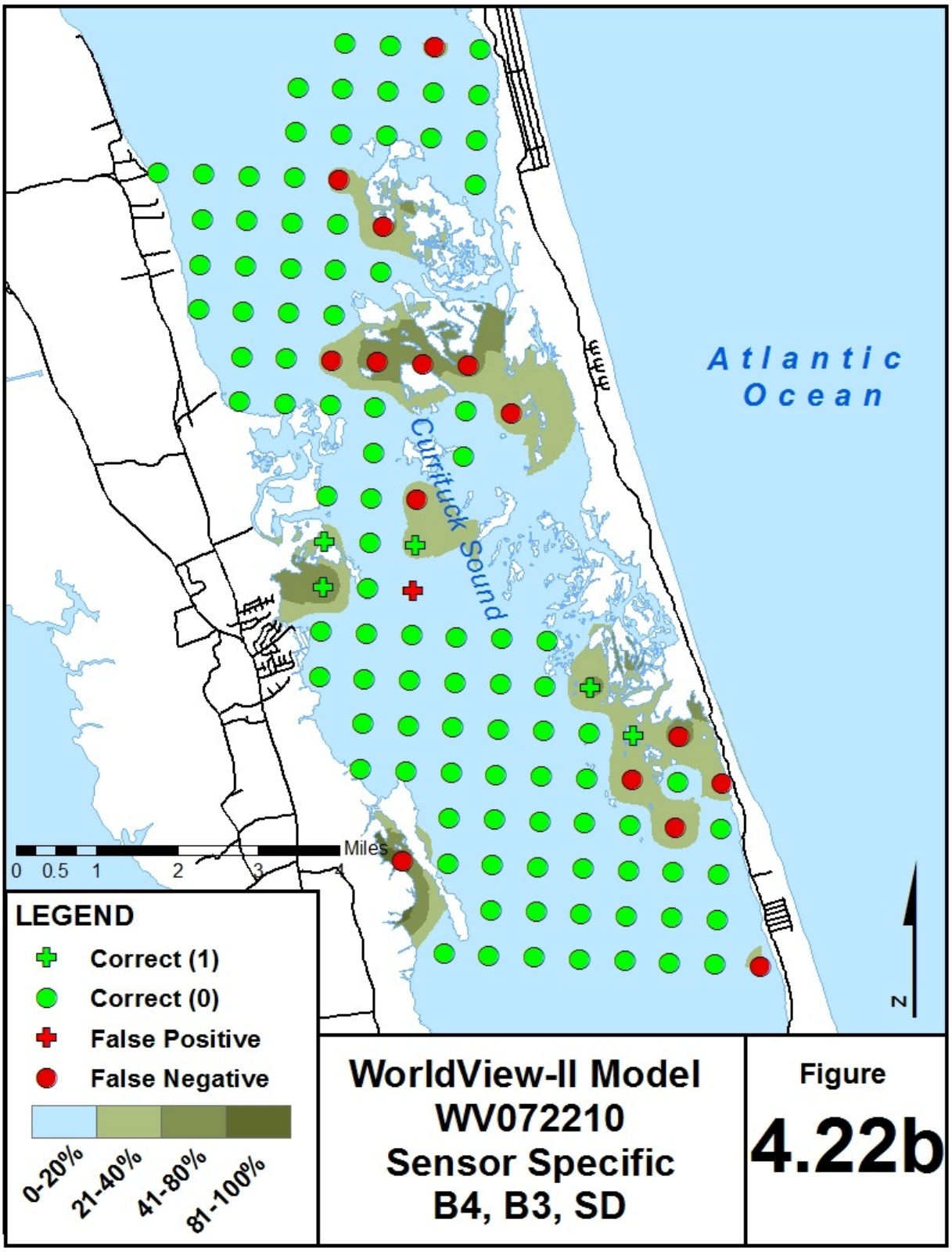

Figure 4.22b. Worldview-II sensor specific model predictions applied to image taken on 07/22/10 and overlain with SAV percent cover estimations from ground truthing run 1.

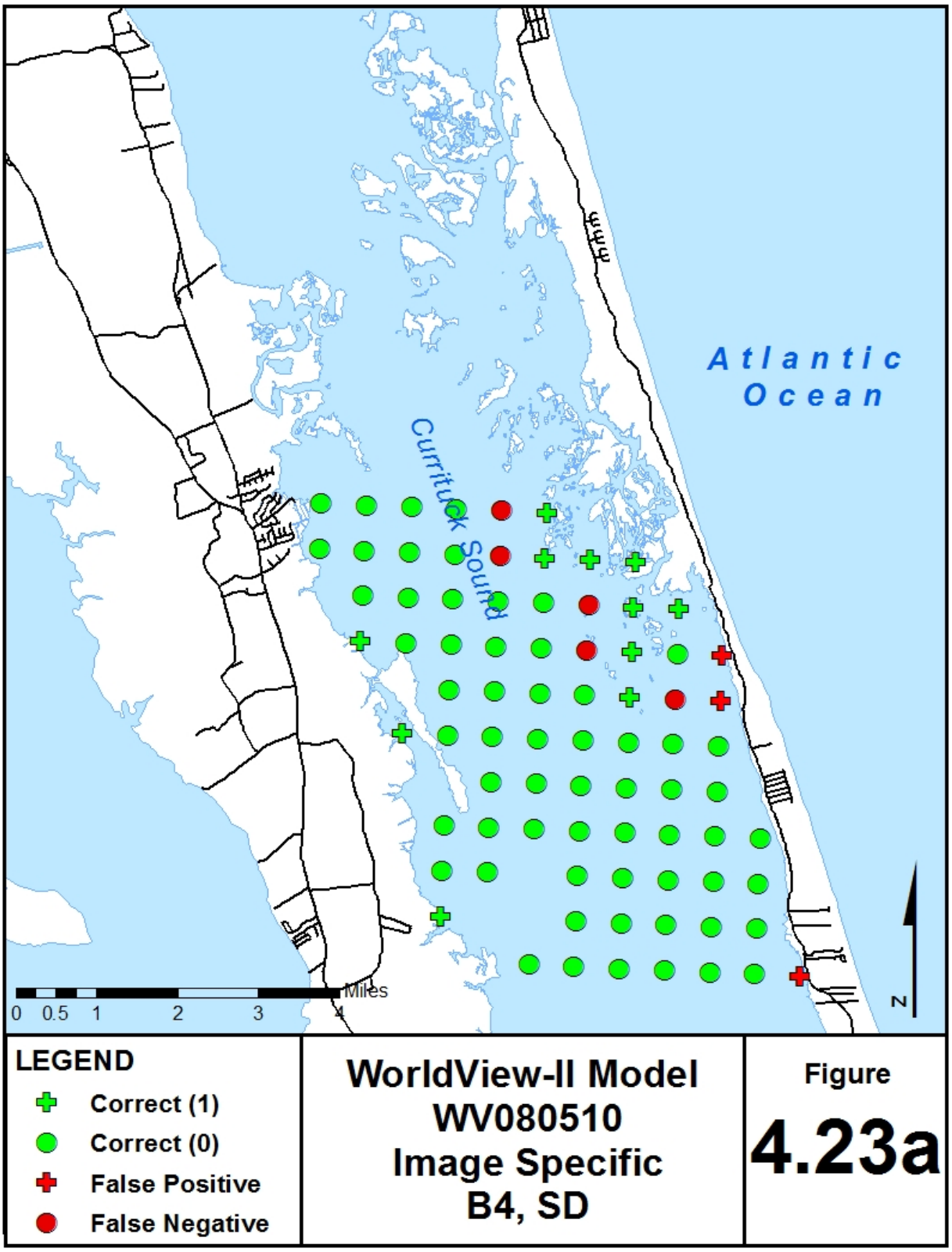

Figure 4.23a. Worldview-II image specific model predictions applied to image taken on 08/05/10.

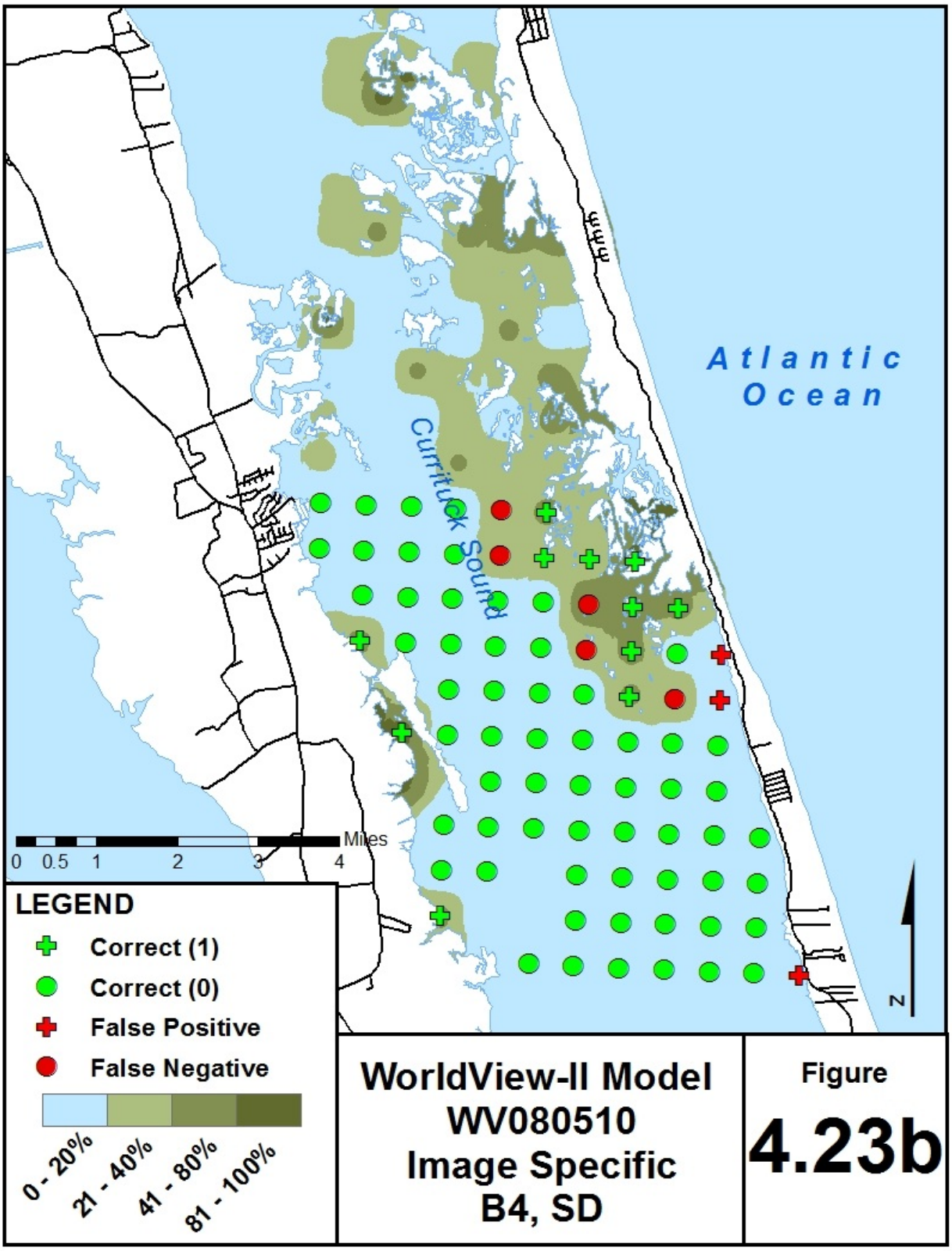

Figure 4.23b. Worldview-II image specific model predictions applied to image taken on 08/05/10 and overlain with SAV percent cover predictions from ground truthing run 2.

4.5.2. Quickbird

The Quickbird sensor derived predictive model yielded a percent concordant value of 73.1% with a Wald of 0.04, Score of 0.0097 and a Likelihood ratio of 0.0175. The most influential predictor variable was band 3 alone, followed by the interaction of band 2 and secchi depth, band 3 and secchi depth, band 2 alone, and a small influence provided by the interaction between band 4 and depth. The positive β coefficient for band 3 alone is consistent with knowledge of the reflective properties of submersed plants in wavelengths from 600 to 700 nanometers. The negative β coefficient associated with band 2 alone is consistent with knowledge of the reflective properties of submersed plants in wavelengths from 520 to 600 nanometers. The positive β coefficient for the interaction between band 2 and secchi depth is consistent with knowledge of the reflective properties of submersed plants in wavelengths from 520 to 600 nanometers and the fact that light penetration decreases as secchi depth increases. The negative β coefficient associated with the interaction of band 3 and secchi depth is consistent with both the reflective properties of plants in wavelengths from 600 to 700 nanometers and the association that light penetration decreases as secchi depth increases. Lastly, the negative β coefficient associated with the interaction of band 4 and depth is consistent with knowledge of submersed plant reflection in wavelengths from 700 to 1000 nanometers and the fact that light penetration decreases as depth increases. Unfortunately, the reliability of this model is in question due to the lag time between image acquisition and field sampling (+ 36 days). Parameter estimates for the Quickbird derived model can be found in tables 4.7. The sensor specific model prediction outputs for the Quickbird sensor can be found in figure 4.24a as well as a comparison of ground truthed SAV estimation to prediction output in figure 4.24b.

Analysis of Maximum Likelihood Estimates					
Parameter	DF	Estimate	Standard Error	Wald Chi-Square	Pr > ChiSq
Intercept	1	1.8684	0.3393	30.3157	<.0001
B2	1	-11.4288	5.4478	4.401	0.0359
B3	1	12.4367	5.373	5.3576	0.0206
B2*SD	1	31.7167	14.3848	4.8615	0.0275
B3*SD	1	-30.4846	14.0404	4.7141	0.0299
B4*D	1	-0.2457	0.1221	4.0476	0.0442

Table 4.7. Parameter estimates for the Quickbird sensor specific model applied to the 09/13/10 dataset.

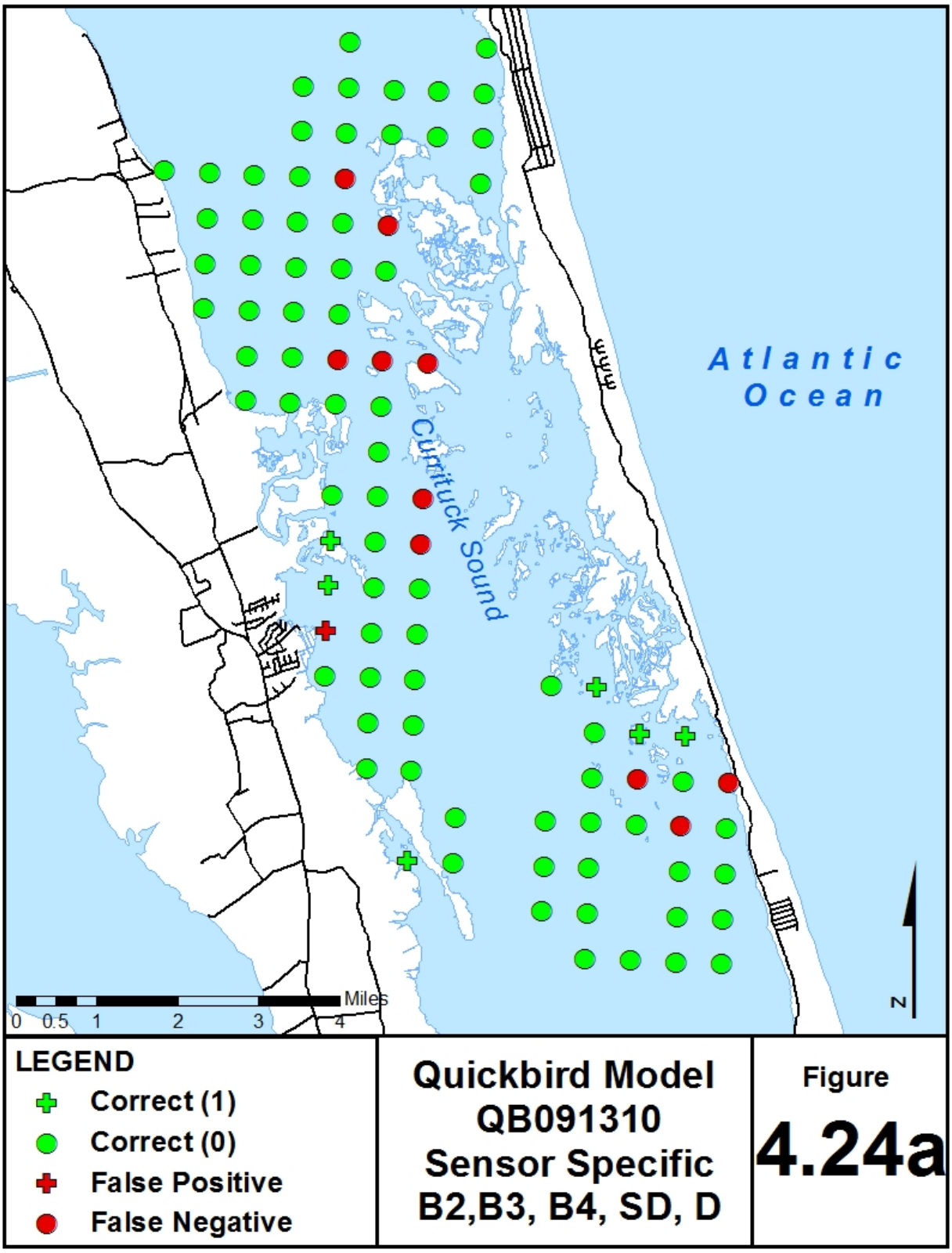

Figure 4.24a. Quickbird sensor specific model predictions applied to image taken on 09/13/10.

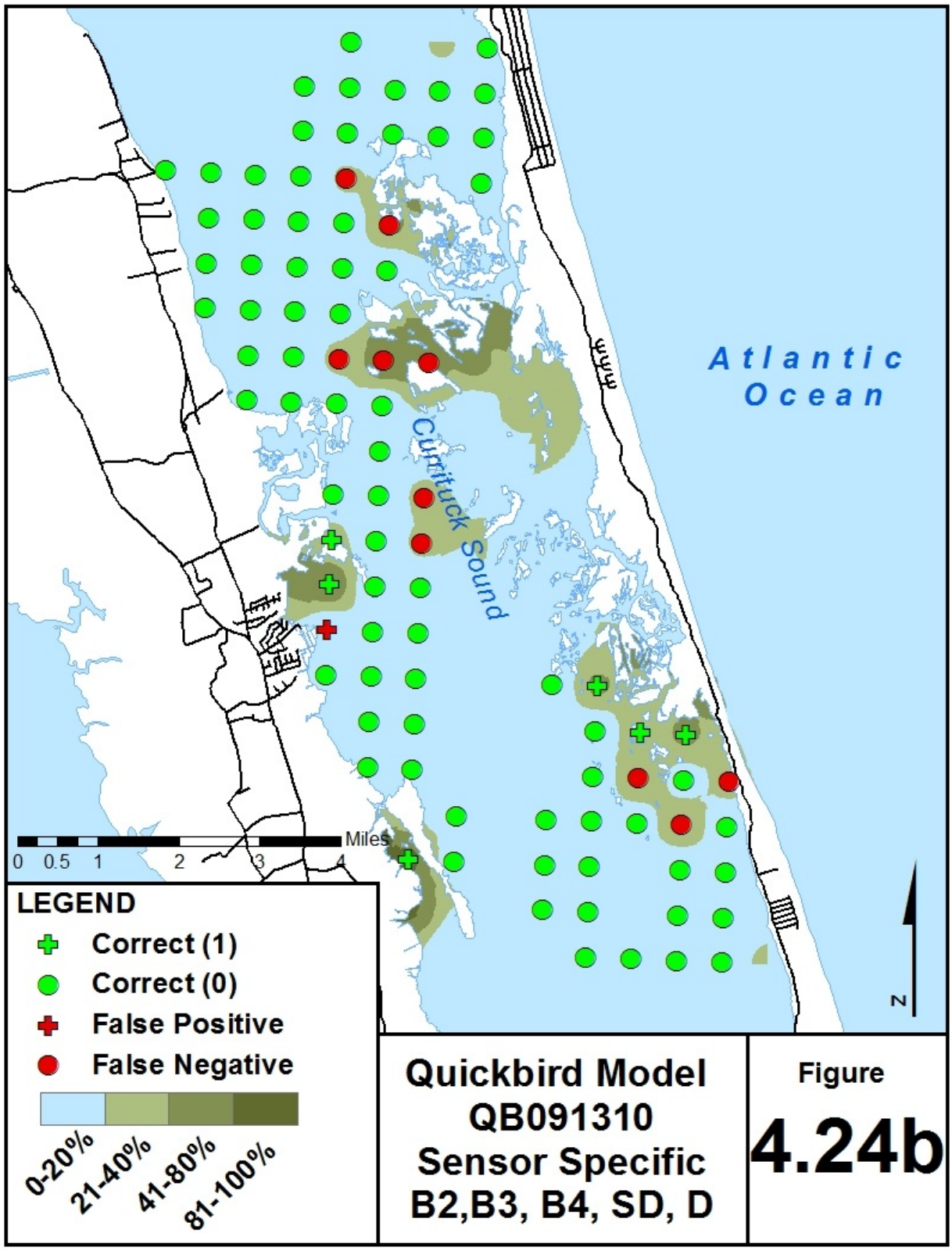

Figure 4.24b. Quickbird sensor specific model predictions applied to image taken on 09/13/10 and overlain with SAV percent cover predictions from ground truthing run 2.

4.3.3. LANDSAT-5

The LANDSAT-5 derived models yielded inconsistent results often varying from scene to scene and suggesting various bands not historically associated with plant reflectance. Although a number of images were available for analysis, a number of these images were affected by clouds, atmospheric haze, and sun-glint. The coarser spatial resolution of LANDSAT-5 imagery also hindered attempts to contain only plant growth within individual pixels. Pixels most likely contained plant matter but also received spectral contribution from background features such as bare bottom.

5. CONCLUSIONS

5.1. Assessment of Methodology

The main objective of this study was to develop and test satellite remote sensing to be used in long-term monitoring of submerged aquatic vegetation. The methodologies utilized in this study were effective in mapping the current extent, distribution and interseasonal variation of submerged aquatic vegetation in the Currituck Sound, NC. The utilization of field sampling gives adequate spatial representation of all variables collected including those relative to SAV distribution, presence, and dominance throughout the summer growing season of 2010. Remote sensing methods utilized multiple sensor images acquired during the 2010 summer growing season, orthorectification of images, extraction of digital numbers into point datasets, and extensive ground reference data culminated into more than 300 total data points. These methods were appropriate for mapping the distribution of submerged aquatic vegetation in the Currituck Sound. Vegetated and non-vegetated areas were accurately mapped using a combination of inverse distance weighted and predictive LOGIT models. Distribution of individual species was distinguished based mainly on the ground reference data. The overall methods were based on widely accepted methods (Nelson 2006, Madsen 1999) with few adaptations based on professional judgment. This study was carried out in its entirety by NCSU employees with contracted services for obtaining satellite imagery for both the Worldview-II and Quickbird sensors. At this point in time, a marriage of traditional SAV mapping techniques and remote sensing are probably the best approach to quantifying SAV status, distribution on a large regional scale. Appropriate avoidance and mitigation can be determined using the methodology described in this study. Individual processes of this study will be addressed in the below paragraphs.

5.2. SAV Field Sampling Utilizing the Point-Intercept Method

5.2.1. Methodology to Determine SAV Status

Field sampling provided the majority of information relative to species specific data and other important variables including depth, secchi depth, sediment type, temperature, salinity and various water quality aspects. All of the variables collected in field sampling

were utilized in one way or another to address model development or to better understand intricate ecological relationships occurring within the Currituck Sound.

5.2.2. Current Status of SAV in the Currituck Sound

At this point, SAV distribution within the sound seems vast, however the density of these SAV beds may be rather low on average. For example, plant coverage category 3 (81-100% coverage) makes up less than 3% of all points surveyed and the majority of those points were inhabited by non-native, Myriophyllum spicatum. Field sampled species data and historical records suggest that species evenness may also have declined in recent years. Beneficial species such as Vallisneria americana and Potamogeton perfoliatus that once shared equal numbers with other native species now make up less than 5% of all vegetated points. Myriophyllum spicatum, the sole invasive species reported to inhabit the Sound, inhabits almost 40% of vegetated points.

5.2.3. Variables Collected

There are a number of variables collected during field sampling that may determine the status and distribution of SAV in the Currituck Sound. SAV and depth seem to share the most significant relationship as has been documented by other studies (Kemp et al. 2004) SAV may also be influenced by fluctuations in salt content of the water as is described in the results of this study. Salinity levels may not be consistently high in most areas of the Sound, however fluctuations may be affecting the overall survivability of SAV within the Mid-Currituck portion of the Sound sampled in this study. Sediment type also seems to play an important role in the location and coverage of SAV. Sandy bottoms most often do not contain any SAV growth.

Other variables of interest utilized but not included in this report are measures of water quality in the sound. Water quality was collected between each sample run and included a number of parameters. It was discovered later in our work that some of these variables shared significant relationships with SAV presence or absence. For example, measures of Total Nitrogen (Figure 5.1) were found to be highly correlated with areas of SAV presence. Because these variables didn't necessarily improve the quality of the logistic models described in this study, they were not included, but should be considered in future work when establishing relationships of SAV to environmental factors.

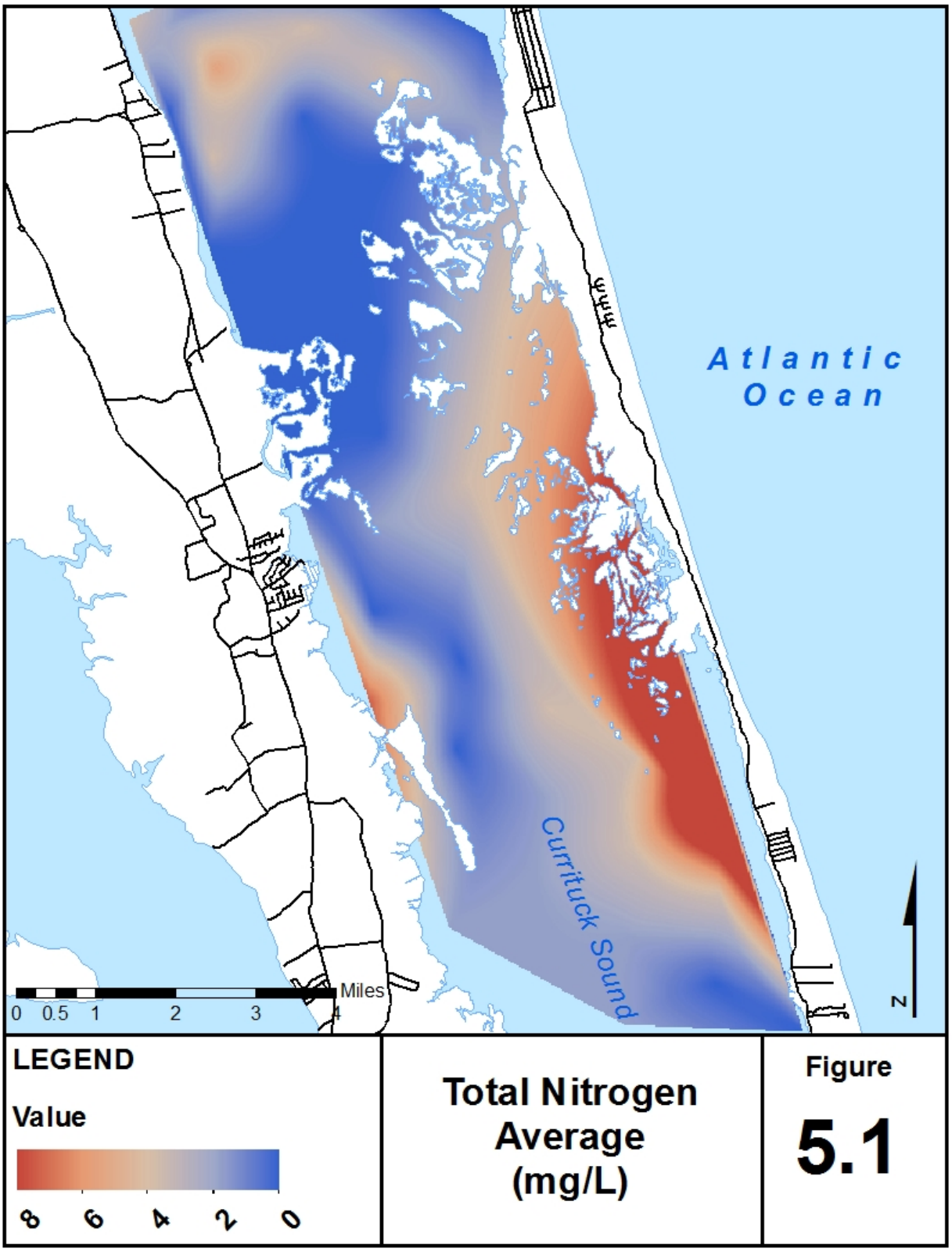

Figure 5.1. Average total Nitrogen for the Study area as estimated during two water quality sampling runs during SAV sampling summer 2010.

5.2.4. Improving on Existing Field Collection

Field sampling could be improved should more personnel and resources be available to do so. As with any aspect of science, repetition and increasing sample sizes can be beneficial to more adequately describing the target of interest. SAV communities could be more adequately mapped in the Currituck Sound given more time and available personnel to increase the spatial resolution or coverage of sampling. The addition of data points would create a smoother and more accurate map of SAV within the Currituck Sound while applying the same methods developed in the study. SAV distribution, density and coverage can potentially be more adequately described if such intense sampling is feasible in the future. Additionally, other variables of interest when considering future development of remote sensing ground truth datasets are: depth to vegetated canopy, length of longest stem, and status of SAV community. Depth to vegetated canopy could influence the ability of sensors to detect growing SAV communities. Plant material located on the surface of the water reflects higher amounts of energy than does plants found deeper in the water column. Length of longest stem could provide insight on the growth of plants between sample runs that may influence sensor detection capability during lag times between sampling runs. Status of SAV community can provide valuable information on the photosynthetic activity of the plants. Dying communities most likely will not contain the same reflective potential as actively growing plants, therefore the status of each community should be noted to determine if there are differences in reflectivity based on the status of the plants at time of data collection.

5.3. Remote Sensing of SAV

5.3.1. Sensor Performance

Remote sensing of SAV in the Currituck Sound is possible at this point, however much more work need be done before developing models of SAV density or extending models beyond the Currituck Sound. Overall, the Worldview-II sensor provided the best predictive model of SAV presence or absence. A percent concordant value greater than 80% is considered to be sufficient when developing predictive models (Nelson et al 2003). Models derived from the Worldview-II sensor consistently produced accurate predictive outputs based on the ground-truthed field data. False positives using the Worldview-II derived models, although few, were most often experienced in areas of shallow depth (<3 feet) (see figure 5.2). This could be due to reflective contribution from bottom sediment, however it should also be noted that four out of the seven false positives experienced across all images with the Worldview-II sensor actually took place at points with at least some SAV present (1-20%). The >20% threshold used to develop the models designated these points as “absent” of SAV, because these points fell below the threshold and were thus designated as points of SAV absence. Future work should

attempt to develop a more applicable threshold for NC coastal bodies of water. False negatives were most often experienced in areas of lower plant density (<40%) or in areas of deeper water (>4 feet). Perhaps spectral contribution of SAV was inhibited by greater distances between plant canopy and water surface. Lower densities of SAV may also not provide an adequate spectral contribution to be differentiated from the water column alone. Plant coverage of an area may also have contributed to false negatives in that SAV coverage in the area extracted from satellite imagery may not have covered an adequate amount of each pixel area for detection.

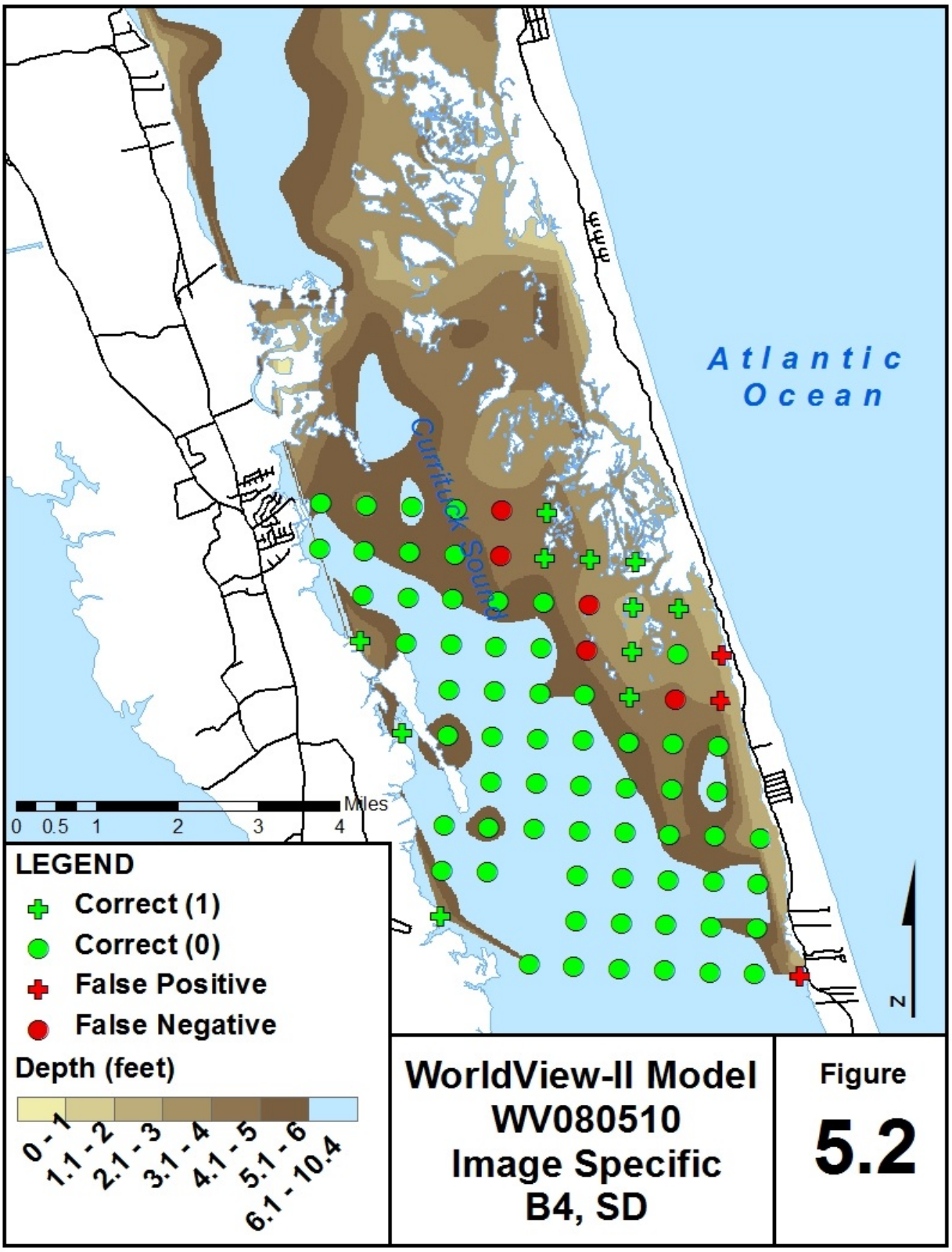

Figure 5.2. Worldview-II image specific model compared to depth profile of the study area.

The Quickbird sensor provided mixed results. With a total of 10 false negatives and 1 false positive, and a percent concordant value of 73.1%, the Quickbird sensor may not be the best sensor for modeling SAV presence or absence in the Currituck Sound. A severe lag in image acquisition date and near-coincidental field sampling most likely contributed to issues with model development as well as a large amount of cloud cover in the Quickbird image (Figure 5.3). Most false negatives experienced in the image were located along a large cloud extending from the southern to northern reach of the study area. Atmospheric interference inherent around clouds can severely alter the spectral signature of the target thus leaving even points not directly within the cloud at risk for contamination.

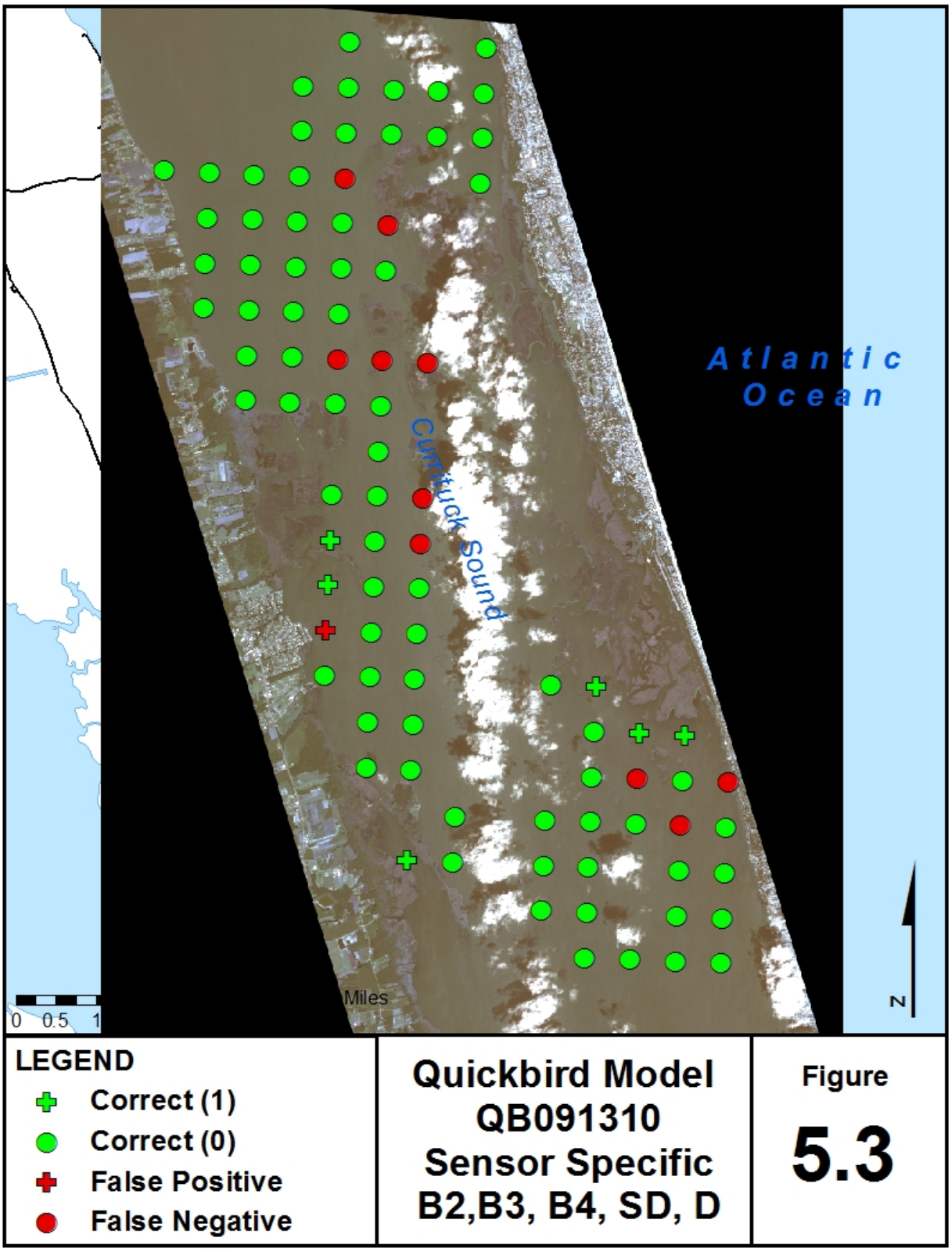

Figure 5.3. Quickbird sensor specific model predictions applied to image taken on 09/13/10 overlain with image.

Although three models were developed with somewhat different influence from each predictor chosen, common variables emerged from each Worldview-II model as well as the Quickbird Model; Band 4 and Secchi Depth. These two predictor variables were utilized in each model and should be investigated first in future attempts at remote sensing of SAV with the WorldView-II sensor. The reflective properties of plants in the Near-Infrared portion of the electromagnetic spectrum have been cited in numerous papers regarding aquatic plants (Nelson 1983, Everitt and Yang 1999). This portion of the spectrum should always be considered when remote sensing of SAVs is desired with the Worldview-II sensor. The spatial resolution of the Worldview-II sensor also made it possible to more adequately capture the sample area from which the ground truth data are based. This became the major limitation to using free LANDSAT 5 data. The sensors 30 meter spatial resolution most likely allowed spectral influence from sources outside of the target SAV. Although LANDSAT 5 imagery have been used in the past for remote sensing of SAV, the patchy distribution of SAV in the Currituck Sound requires high spatial resolution imagery for remote sensing of SAV presence/absence at this time.

5.3.2. Issues Experienced

Complications arose using all sensors due to the low occurrence of events to non-events in the ground-truthed data. As is mentioned earlier, logistic regression requires that events, in this case SAV presence, to constitute 30% of the dataset. This qualification was met for SAV presence/absence in the Sound and as such, a model of SAV presence/ absence was developed. In the case of SAV percent coverage, the occurrence of events to non-events per class was very low. SAV density was inversely proportional to number of points per coverage class. The areas most likely to be detected by remote sensing (Class 3: 81-100%) were the least often to occur. This made modeling of SAV percent coverage impossible given the lack of dense stands of SAV in the Currituck Sound. Increasing the sample size was suggested after the fact, but in the case of the Currituck Sound, this would actually compound the negative effect of the ratio of events to non-events that occurred during sampling previously. Remote sensing of SAVs in percent coverage class limited bodies of water or bodies of water lacking large representation of higher percent coverage classes should be done with caution.

Poor performance in image acquisition led to less than ideal acquisition dates. Originally, images were scheduled to be taken as near to actual dates of field sampling as possible. Actual acquisition dates lagged and time between sample run 1 and image acquisition left the utility of sample run 1 as a ground truthed dataset questionable. This is especially true with the Quickbird image acquired in mid-September, leaving sample run 1 unusable for model development using this sensor. Only sample run 2 and validation sample run 3 were used to develop a model for the Quickbird sensor. Future attempts to replicate this study should take special care to schedule and obtain imagery from dates as near-coincidental as possible to actual SAV sampling.

5.4. Future Work

Remote sensing has proven to be a promising tool for detecting SAV within the Currituck Sound and potentially into similar water bodies despite many complications and setbacks during the course of this study. As is mentioned earlier, the Currituck Sound has a low ratio of events (SAV presence) to non-events (SAV absence), thus complicating model development using the logistic regression approach. On the contrary, perhaps bodies of water with many points containing SAV representing a range of plant coverage may prove more successful for application of remote sensing. Concern for invasion by invasive species in NC water bodies is becoming more of an issue with each passing year. Invasive submersed plant species such as Hydrilla verticillata (Hydrilla), Egeria densa (Brazilian Elodea), and Najas minor (Brittle naiad) already have a foothold in many waterbodies of the state and have begun to move into neighboring waterbodies to the Currituck Sound in recent years. These invasive species are known for their dense canopies and large coverage areas once established in a body of water. Given that remote sensing shows such promise for the ability to model SAV presence absence even in SAV poor bodies of water, the next logical step would be in attempting to model SAV in plant rich bodies of water. Unfortunately, these bodies of water are most often those that are inundated with invasive species such as those mentioned above. Future work should include the investigation of remote sensing as a tool to track species changes, percent coverage of SAV and SAV ranges in NC coastal bodies of water.

Sediment change through disturbance is also a key component to monitoring SAV. Although not included in model development, there was substantial evidence that sediment type and SAV presence or absence is related. Areas of sand most often did not contain any SAV. During this study, we found that sediment type actually changed from the early summer sampling to late summer sampling in at least 5 points. Understanding the roll of disturbance in identifying potential areas of SAV colonization should be of utmost importance in future studies. Sediment type plays a key role in the establishment of aquatic plants and this can be altered greatly by disturbance events such as hurricanes (Rodusky 2010). Given that the Currituck Sound has undergone two major disturbance events in the past two years (Hurricane Irene 2011 and Hurricane Sandy 2012), the impacts of these storms must be assessed to determine the effect that sediment change has on SAV communities.

As existing sensors continue to be improved and new sensors developed, the ability of the NCDOT to utilize remote sensing for mapping and monitoring will continue to improve. Additionally, continued exploration of the spectral characteristics of different submersed aquatic plant communities is of utmost importance to improve the models developed in this study. Presently, the Worldview-II sensor and Quickbird sensor, coupled with traditional field sampling techniques, provide an excellent means to map and monitor SAVs in the Currituck Sound.

6.0. REFERENCES

Ackleson, S.G., Klemas, V., 1987. Remote-sensing of submerged aquatic vegetation in lower Chesapeake Bay: a comparison of Landsat MSS to TM imagery. Remote Sens. Environ. 22, 235–248.

Armstrong, R., 1993. Remote sensing of submerged vegetation canopies for biomass estimation. Int. J. Remote Sens. 14, 621–627.

Crumpton, W.G., Isenhart, T.M., Mitchell, P.D., 1992. Nitrate and organic N analysis with 2nd-derivative spectroscopy. Limnol. Oceanogr. 37, 907–913.

Dekker, A.G., Peters, S.W.M., 1993. The use of the Thematic Mapper for the analysis of eutrophic lakes: a case study in the Netherlands. Int. J. Remote Sens. 14, 799–821.

Everitt, J.H. and Yang, C. and Escobar, D.E. and Webster, C.F. and Lonard, R.I. and Davis, M.R. (1999) Using Remote Sensing and Spatial Information Technologies to Detect and Map Two Aquatic Macrophytes. Journal of Aquatic Plant Management, 37, pp. 71-80.

Ferguson, R.L., Korfmacher, K. (1997). Remote sensing and GIS analysis of seagrass meadows in North Carolina, USA. Aquatic Botany, 28, 241-258.

Hosmer D.W. and Lemeshow S., 2000. Applied logistic regression, 2nd ed. New York: John Wiley &. Sons, Inc,. ISBN 0-471-35632-8.

Jensen, J.R., Narumanlani, S., Weatherbee, O., Mackey Jr., H.E., 1993. Measurement of seasonal and yearly cattail and waterlily changes using multidate SPOT panchromatic data. Photogramm. Eng. Remote Sens. 52, 31–36.

Kemp,M.W., Batiuk, R., Bartleson, R., Bergstrom, P., Carter, V.,Gallegos, C.L., Hunley, W., Karrh, L., Koch, E.W., Landwehr, J.M., Moore, K.A., Murray,L., Naylor, M., Rybicki, N.B., Stevenson, J.C. and D.J. Wilcox. Habitat Requirements for Submerged Aquatic Vegetation in Chesapeake Bay: Water Quality, Light Regime, and Physical-Chemical Factors. *Estuaries* , Vol. 27, No. 3 (Jun., 2004), pp. 363-377

Kleinbaum, D.G., 1994. Logistic Regression A Self-learning Text. Springer-Verlag Publishing, New York.

Kloiber, S.M., Anderle, T.H., Brezonik, P.L., Olmanson, L., Bauer, M.E., Brown, D.A., 2000. Trophic state assessment of lakes in the Twin Cities (Minnesota USA) region by satellite imagery. Archiv. Hydrobiologie Special Issues Adv. Limnol. 55, 137–151.

Khorram, S., Cheshire, H.M., 1985. Remote sensing of water quality in the Neuse River Estuary North Carolina. Photogramm. Eng. Remote Sens. 51, 329–341.

Lathrop, R.G., Lillesand, T.M., 1986. Utility of Thematic Mapper data to assess water quality. Photogramm. Eng. Remote Sens. 52, 671–680.

Lehmann, A., Lachavanne, J.B., 1997. Geographic information systems and remote sensing in aquatic botany. Aquat. Bot. 58, 195–207.

Lillesand, T.M., Johnson, W.L., Deuell, R.L., Linstrom, O.M., Meisner, D.E., 1983. Use of Landsat data to predict the trophic state of Minnesota lakes. Photogramm. Eng. Remote Sens. 49, 219–229.

Lillesand, T.M., Kiefer, R.W., 1994. Remote Sensing and Image Interpretation. John Wiley and Sons, Inc., New York.

Madsen, J.D., 1999. Point intercept and line intercept methods for aquatic plant management. Army Corps of Engineers Waterways Experiment Station Technical Note MI-02.

Marshall, T.R., Lee, P.F., 1994. Mapping aquatic macrophytes through digital image analysis of aerial photographs: assessment. J. Aquat. Plant Manage. 32, 61–66.

Menzel, D.W., Corwin, N., 1965. The measurement of total phosphorus in seawater based on the liberation of organically bound fractions by persulfate oxidation. Limnol. Oceanogr. 10, 280–282.

Murphy, J., Riley, L.P., 1962. A modified single solution method for the determination of phosphate in natural waters. Anal. Chimica Acta 27, 31–36.

Narumalani, S., Jensen, J.R., Althausen, J.D., Burkhalter, S.G., Mackey Jr., H.E., 1997. Aquatic macrophyte modeling using GIS and logistic multiple regression. Photogramm. Eng. Remote Sens. 63, 41–49.

Nelson, R.F., 1983. Detecting forest canopy change due to insect activity using Landsat MSS, Photogrammetric Engineering & Remote Sensing, 49:1303-1314.

Nelson, S.A.C., Soranno, P.A., Cheruvelil, K.S., Batzli, S.A., Skole, D.L., 2003. Regional assessment of lake water clarity using satellite remote sensing. J. Limnol. 62 (Suppl. 1), 27–32.

Orth, R.J., Moore, K.A., 1983. Submerged vascular plants: techniques for analyzing their distribution and abundance. Mar. Technol. Soc. J. 17, 38–52.

Pampel, F.C., 2000. Logistic Regression: A Primer. Sage University Papers Series Quantitative Applications in the Social Sciences, series no. 07-132. Sage Publications, CA.

Penuelas, J., Gamon, J.A., Griffen, K.L., Field, C.B., 1993. Assessing coummunity type, plant biomass, pigment composition, and photosyntheic efficiency of aquatic vegetation on spectral reflectance. Remote Sens. Environ. 46, 110–118.

Raitala, J., Lampinen, J., 1985. A Landsat study of the aquatic vegetation of the lake Luodonjarvi reservoir Western Finland. Aquat. Bot. 21, 321–346.

Rodusky, Andrew J. 2010. The Influence of Large Water Level Fluctuations and Hurricanes on Periphyton and Associated Nutrient Storage in Subtropical Lake Okeechobee, USA. Aquatic Ecology 44.4: 797-815. Web.

Wicker A.M., Endres K.M. 1995. Relationship between waterfowl and American Coot abundance with submersed macrophytic vegetation in Currituck Sound, North Carolina. Estuaries, 18(2) 428-431.

Sincock, J.L., K.E. Johnston, J.L. Coggin, R.E.Wollitz, J.A. Kerwin, and J. Grandy. 1965. Back Bay – Currituck Sound data report. U.S. Fish and Wildlife Service, North Carolina Wildlife Resources Commission, and Virginia Commission of Game and Inland Fisheries. 1600 pp.

Valley, R.D., Drake, M.T., Anderson, C.S., 2005. Evaluation of alternative interpolation techniques for the mapping of remotely-sensed submersed vegetation abundance. Aquat. Bot. 81, 13–25.

Verbyla, D.L., 1995. Satellite Remote Sensing of Natural Resources. CRC Lewis Publishers, New York.

Vis, C., Hudon, C., Carignan, R., 2003. An evaluation of approaches used to determine the distribution and biomass of emergent and submerged aquatic macrophytes over large spatial scales. Aquat. Bot. 77, 187–201.

Zhang, X., 1998. On the estimation of biomass of submerged vegetation using Landsat Thematic Mapper (TM) imagery: a case study of the Honghu Lake, PR China. Int. J. Remote Sens. 19, 11–20.

Zilioli, E., 2001. Lake water monitoring in Europe by means of remote sensing. Sci. Total Environ. 268, 1–2.